Science of the Total Environment 634 (2018) 1004–1023

Contents lists available at ScienceDirect

Science of the Total Environment

journal homepage: www.elsevier.com/locate/scitotenv

Permafrost thaw and climate warming may decrease the CO_2, carbon, and metal concentration in peat soil waters of the Western Siberia Lowland

T.V. Raudina [a], S.V. Loiko [a], A. Lim [a], R.M. Manasypov [a,b], L.S. Shirokova [b,c], G.I. Istigechev [a], D.M. Kuzmina [a], S.P. Kulizhsky [a], S.N. Vorobyev [a], O.S. Pokrovsky [c,*]

[a] BIO-GEO-CLIM Laboratory, Tomsk State University, Lenina av, 36 Tomsk, Russia
[b] N Laverov Federal Center for Integrated Arctic Research, Institute of Ecological Problems of the North, Russian Academy of Science, Arkhangelsk, Russia
[c] Geoscience and Environment Toulouse (GET), UMR 5563 CNRS University of Toulouse, 14 Avenue Edouard Belin, 31400 Toulouse, France,

HIGHLIGHTS

- Lack of decrease of DOC, CO_2, and CH_4 concentrations in active layer waters with latitude and permafrost coverage.
- Potential of GHG emission from soil water does not decrease with the increase in permafrost coverage.
- The climate warming in western Siberia may lead to northward migration of the permafrost boundary and change of microlandscapes.
- This might not sizably impact the GHG regime, dissolved carbon, and trace metal content in surface waters of frozen peatlands.

GRAPHICAL ABSTRACT

Shift of the permafrost boundary northward due to climate warming may decrease, not increase the GHG, DOC, and metal concentration in peat soil waters and riverine export fluxes.

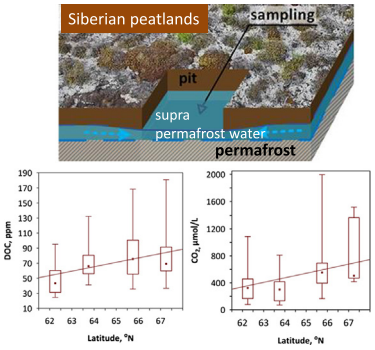

ARTICLE INFO

Article history:
Received 24 October 2017
Received in revised form 5 April 2018
Accepted 5 April 2018
Available online 11 April 2018

Keywords:
Carbon dioxide
Methane
Suprapermafrost flow
Permafrost table
Peat
River
Climate warming

ABSTRACT

Soil pore waters are a vital component of the ecosystem as they are efficient tracers of mineral weathering, plant litter leaching, and nutrient uptake by vegetation. In the permafrost environment, maximal hydraulic connectivity and element transport from soils to rivers and lakes occurs via supra-permafrost flow (i.e. water, gases, suspended matter, and solutes migration over the permafrost table). To assess possible consequences of permafrost thaw and climate warming on carbon and Green House gases (GHG) dynamics we used a "substituting space for time" approach in the largest frozen peatland of the world. We sampled stagnant supra-permafrost (active layer) waters in peat columns of western Siberia Lowland (WSL) across substantial gradients of climate (−4.0 to −9.1 °C mean annual temperature, 360 to 600 mm annual precipitation), active layer thickness (ALT) (>300 to 40 cm), and permafrost coverage (sporadic, discontinuous and continuous). We analyzed CO_2, CH_4, dissolved carbon, and major and trace elements (TE) in 93 soil pit samples corresponding to several typical micro landscapes constituting the WSL territory (peat mounds, hollows, and permafrost subsidences and depressions). We expected a decrease in intensity of DOC and TE mobilization from soil and vegetation litter to the supra-permafrost water with increasing permafrost coverage, decreasing annual temperature and ALT along a latitudinal transect from 62.3°N to 67.4°N. However, a number of solutes (DOC, CO_2, alkaline earth metals, Si, trivalent and tetravalent hydrolysates, and micronutrients (Mn, Co, Ni, Cu, V, Mo) exhibited a northward increasing trend with highest concentrations within the continuous permafrost zone. Within the "substituting space for

* Corresponding author.
E-mail address: oleg.pokrovsky@get.omp.eu. (O.S. Pokrovsky).

https://doi.org/10.1016/j.scitotenv.2018.04.059
0048-9697/© 2018 Elsevier B.V. All rights reserved.

time" climate change scenario and northward shift of the permafrost boundary, our results suggest that CO_2, DOC, and many major and trace elements will decrease their concentration in soil supra-permafrost waters at the boundary between thaw and frozen layers. As a result, export of DOC and elements from peat soil to lakes and rivers of the WSL (and further to the Arctic Ocean) may decrease.

© 2018 Elsevier B.V. All rights reserved.

1. Introduction

Biogeochemistry of carbon and related elements in surface waters of permafrost regions is an actively expanding field in scientific research that is chiefly motivated by need for quantitative prediction of aquatic and soil ecosystem response to on-going permafrost thaw (Johnson et al., 2013; Čapek et al., 2015; Schuur et al., 2015; Vonk et al., 2015; Grosse et al., 2016). The main factor controlling elemental behavior during accelerating thaw in permafrost and release of soil carbon and metals to surrounding aquatic landscapes is the connectivity between soils and rivers or lakes, which occurs via water and solute transport along the permafrost table ("supra-permafrost flow"). The supra-permafrost (shallow subsurface) water occurs in the active layer, typically at the border between the thawed and frozen part of the soil profile (Woo, 2012). In the permafrost regions having no groundwater discharge, this water represents a major source of solutes to rivers or lakes from surrounding soils. Accordingly, in soil ecosystems, the main impact of climate change such as accelerating chemical weathering (Keller et al., 2010; Beaulieu et al., 2012) via active layer thickness rise (Zhang et al., 2005; Akerman and Johansson, 2008), productivity and plant biomass (Abbott et al., 2016; Ziegler et al., 2017), or change in precipitation regime (Walvoord and Kurylyk, 2016) and subsurface water travel time (Frampton and Destouni, 2015) will be transferred to aquatic ecosystems via this supra-permafrost water flux.

However, until now, the majority of research efforts were focused either on aquatic (Giesler et al., 2006, 2014; Guo et al., 2007; Olefeldt and Roulet, 2012; Quinton and Baltzer, 2013; Olefeldt and Roulet, 2012) or terrestrial (Johnston et al., 2014; Hodgkins et al., 2014; Liu et al., 2016; Yang et al., 2016) components of continental permafrost-bearing ecosystems. Relatively few studies address the biogeochemistry of soil porewaters, supra-permafrost (active layer) waters, or shallow groundwaters in the permafrost landscapes (Petrone et al., 2006; Jantze et al., 2013; Jessen et al., 2014; Newmann et al., 2015; Street et al., 2016; Throckmorton et al., 2016; Lamhonwah et al., 2017). Most of these studies dealt with mineral rather than organic portions of soil profiles to characterize chemistry of active layer fluids in the permafrost zone. In contrast, a lot of work has been done on DOC and metal behavior in porewaters of boreal and temperate non-permafrost peatlands (i.e., Siegel et al., 1995; Steinmann and Shotyk, 1997; Bendell-Young, 2003; Karavanova and Malinina, 2007; Avagyan et al., 2014; Gangloff et al., 2016; Griffiths and Sebestyen, 2016; Shotyk et al., 2016; Dielemann et al., 2016; Wertebach et al., 2016).

This study aims to fill this gap by analyzing a large suite of supra-permafrost waters from permafrost regions within the western Siberia Lowland (WSL). This is one of the largest frozen peatland provinces in the world and its location is within both discontinuous and continuous permafrost zones. The primary interest for the WSL is that it contains sizeable reservoirs of organic carbon located in active and still thickly frozen (≤5 m) peat layers (Botch et al., 1995; Kremenetski et al., 2003; Frey and Smith, 2007; Beilman et al., 2009; Smith et al., 2004; Tarnocai et al., 2009; Gentsch et al., 2015). Thus, unlike the deep (up to 40 m) yedoma of Eastern Siberia or Alaska, the soil organic matter of the WSL peatlands is highly susceptible to mobilization to aquatic ecosystems similar to non-permafrost settings (Pawson et al., 2012; Palmer et al., 2016) and high-latitude systems (Dean et al., 2016). The impact of climate warming on peatlands of the WSL may be manifested via southern permafrost boundary shift northward (Frey et al. 2007; Sherstyukov and Sherstyukov, 2015), increase in active layer thickness (ALT) (Drozdov et al., 2010; Romanovsky et al., 2010; Moskalenko, 2012; Reshetko and Moiseeva, 2016) and plant productivity (Kirdyanov et al., 2012; Anisimov et al., 2015; Abbott et al., 2016), and increase in river discharge (Yang et al., 2004). In order to foresee the consequences of this impact, we used a "substitution space for time" approach that is fairly well established in the northern regions of the world (Frey et al. 2007; Frey and Smith, 2005; Weyhenmeyer and Karlsson, 2009) and sampled supra-permafrost waters across a 650-km latitudinal profile covering areas of sporadic, isolated, discontinuous, and continuous permafrost. The advantage of this latitudinal gradient in western Siberia is the highly homogeneous landscape parameters and the position of maximal ALT within the peat rather than the mineral horizon. This allows for straightforward testing on the effect of climate, permafrost, and vegetation on soil water chemistry without interference from rock lithology, runoff, relief, proximity to the ocean, and localization of underground waters. Taking advantage of the unique yet boreal plain representative physio-geographical settings in the WSL, we hypothesize that the decreasing concentration of carbon, major and micronutrients in peat porewaters moving northward is related to decrease in vegetation coverage, mean annual temperature, duration of summer season, and the depth of the thawed peat layer. Our specific objectives were to *i*) assess the latitudinal trend of GHG, DOC, major and trace elements in supra-permafrost waters sampled in 4 representative sites in the northern WSL, *ii*) characterize variability of supra-permafrost waters at dominant micro-landscapes (mound, depression and permafrost subsidence), and *iii*) compare the latitudinal trend of soil water components with that observed in rivers and lakes of this region. Addressing these objectives should allow for quantification of possible changes in supra-permafrost and shallow groundwater chemistry over the long-term scenario of climate warming; these objectives will also allow for assessment on the impact of soil processes in surface water chemistry throughout this vast territory of sporadic, discontinuous and continuous permafrost.

2. Study site and methods

2.1. Geographical setting and supra-permafrost water sampling

Sampling was performed along the latitudinal transect of Western Siberia Lowland (WSL) whose northern part is comprised of taiga zone (Kogalym), forest-tundra (Khanymey and Pangody), and tundra (Tazovsky) biomes. The region is within the watershed of the Ob, Nadym, Pur, and Taz rivers which drain Pleistocene sands and clays and are covered by a 1 to 5 m peat layer (Fig. 1 A). Key physio-geographical parameters of studied sites are described in Table 1. The peat was actively forming since the beginning of the Holocene until freezing of bogs in sub-Boreal period (9–4.5 thousands y.a.). After that, the rate of peat formation in bog areas has decreased (Peregon et al., 2007; Vasil'chuk et al., 2008; Panova et al., 2010; Ponomareva et al., 2012; Batuev, 2012). The main mineral substrates underlying frozen peat layers of the WSL are quaternary clays, sands, and alevrolites. In the southern part of the WSL (Kogalym and Khanymey) the typical substrate is sands of lake alluvium origin with rare layers of alevrolites (Klinova et al., 2012). In Pangody the substrate is composed of silts and clays overlaying lake alluvium sands. In Tazovsky the substrate is alluvial sands with alevrolites (Nazarov, 2007). Overall, the mineral

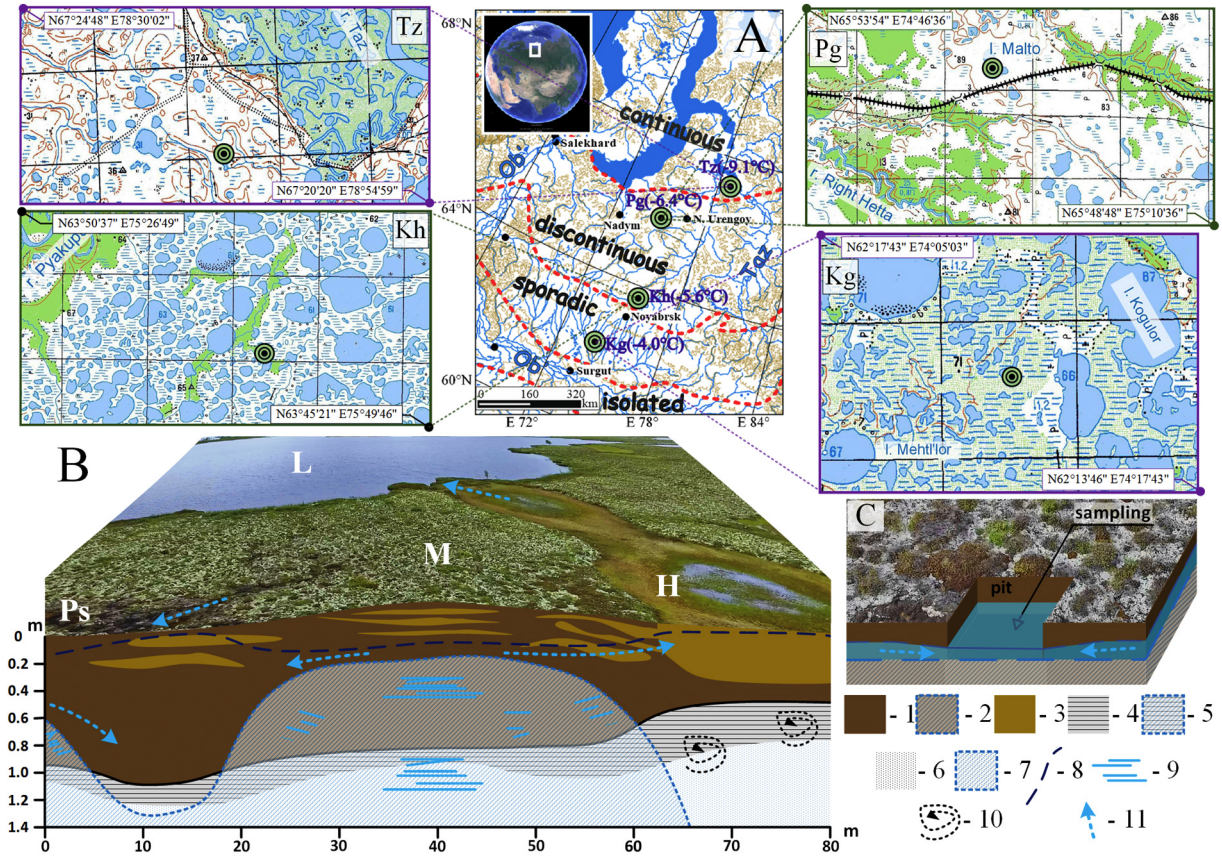

Fig. 1. Study sites and illustration of sampling scheme. **A:** Map of the study site with permafrost boundaries (Brown et al., 2001; http://portal.inter-map.com (NSIDC)), with 4 test sites – Kogalym (Kg), Khanymey (Kh), Pangody (Pg) and Tazovsky (Tz). The square size of the inserts is 1 × 1 km. **B:** A soil and permafrost transect of studied frozen bogs in the Khanymey site, where L is lake; M is peat mound; H is hollow; Ps is permafrost subsidence. **C:** An illustration of water sampling from the pit. Legend: 1, moss-lichen-sedge peat of medium degree of decomposition (Hemic); 2, permanently frozen peat; 3, Sphagnum peat of low degree of decomposition (Fibric); 4, illuvial-humic (spodic) horizon; 5, permanently frozen spodic horizon; 6, sand deposits; 7, frozen sand; 8, the level of supra-permafrost waters in August; 9, ice wedges; 10, cryoturbation features in soil; 11, direction of water flow.

substrates are quite similar among all 5 sites of the northern part of WSL and were subjected to strong influence of aeolian processes in the beginning of the Holocene (Velichko et al., 2011).

Climate ranges from moderately humid and cool in summer to cold and snowy in winter in Kogalym to humid and cold in summer to cold and snow-deficient in winter in Tazovsky. Mean annual temperatures are

Table 1
Physico-geographical and landscape characteristics of 5 study sites cross the permafrost gradient in WSL.

Site	Mean annual temp., °C	Mean annual precipit., mm	Mineral substrate	Micro-landscapes	Share of micro-landscape, %	Peat thickness, m	Seasonal thaw depth, cm	Soil type (WRB, 2014)
Tazovsky, (Tz)	−9.1 °C	363	Clay loam and loam	Polygon	65	2.0–4.0	41	Dystric Hemic Epicryic Histosols (Hyperorganic); Dystric Murshic Hemic Epicryic Histosols (Hyperorganic)
67.4°N 78.7°E				Permafrost subsidences	7		55	Dystric Epifibric Hemic Cryic Histosols (Hyperorganic)
				Frost crack	13		44	Dystric Epifibric Cryic Histosols (Hyperorganic)
				Hollows	16	0.2–1.5	65	Dystric Fibric Cryic Histosols; Histic Reductaquic Cryosols (Clayic)
Pangody, (Pg)	−6.4 °C	484	Loam	Peat mounds	53	0.2–1.3	49	Dystric Hemic Epicryic Histosols; Histic Cryosols (Loamic); Histic Oxyaquic Turbic Cryosols (Loamic)
65.9°N 75.0°E				Permafrost subsidences	10	0.6–1.1	74	Dystric Hemic Endocryic Histosols
				Hollows	37	0.3–1.0	82	Dystric Epifibric Endocryic Histosols; Histic Reductaquic Turbic Cryosols (Loamic); Dystric Fibric Histosols (Gelic)
Khanymey, (Kh)	−5.6 °C	540	Sand	Peat mounds	49	0.1–1.4	90	Dystric Hemic Cryic Histosols; Spodic Histic Turbic Cryosols (Albic, Arenic); Histic Turbic Cryosols (Albic, Arenic)
63.8°N 75.6°E				Permafrost subsidences	30	0.7–1.1	165	Dystric Hemic Histosols (Gelic)
				Hollows	21	0.4–1.1	215	Dystric Epifibric Histosols; Spodic Histic Turbic Cryosols (Arenic); Gleyic Histic Entic Podzols (Turbic)
Kogalym, (Kg) 62.3°N; 74.2°E	−4.0 °C	594	Sand	Ridge	61	1.7–2.3	–	Dystric Ombric Fibric Histosols (Hyperorganic)

−4.0, −5.6, −6.4, and −9.1 °C for Kogalym, Khanymey, Pandogy and Tazovsky, respectively (Trofimova and Balybina, 2014). Permafrost is present at all sites and ranges from discontinuous to sporadic in the south to continuous in the north. Three main micro landscapes probed in this work are present across the latitudinal gradient: peat mounds, hollows, and permafrost subsidences (Fig. 1 B). The average active layer thickness (ALT) at the time of sampling ranged from 200 to 300 cm in the south to 65 cm in the north for hollows whereas mounds (hummocks) ranged from 90 cm in the south to 41 cm in the north.

Vegetation of three studied bog types (polygonal, mound, and ridge-hollow) is essentially oligotrophic (poor in nutrients) which indicates ombrotrophic conditions (i.e. lack of groundwater input and lateral surface influx). The mounds and polygons are covered by dwarf shrubs (*Ledum ssp., Betula nana, Andromeda polifolia, Vaccinium ssp., Empetrum nigrum)*, lichens (*Cladonia ssp., Cetraria, Ochrolechia)* and mosses (*Dicranum ssp., Polytrichum ssp., Sphagnum angustifolium, S. lenense*). Depressions and frost cracks contain moss-sedge associates (grasses *Eriophorum russeolum, E. vaginatum, Carex rotundata, C. limosa, Menyanthes trifoliate, Comarum palustre*; mosses *S. balticum, S. majus, S. lindbergii, S. warnstorfii* and dwarf shrubs *Oxycoccus palustris*). In the most southern site (Kogalym), the pine *Pinus sylvestris* is abundant on ridges (Ilina et al., 1985; Peregon et al., 2007, 2009).

The stagnant supra-permafrost waters (10 at Kogalym, 30 at Khanymey, 28 at Pangody and 35 at Tazovsky) were sampled in August 2015 from a 40 × 40 × 80 cm pit at the active layer – permafrost boundary (Fig. 1C). In mounds and dry depressions, the pit was usually filled by water within 30–60 min after digging. In wet depressions, 20 × 20 × 20 cm pits were filled immediately by surrounding water. The sampling of mounds was always performed in the middle, the highest, part. Note that the surface of depressions is always 0.5 to 0.7 m below that of mounds, and the difference in suprapermafrost water horizon between mounds and depressions is between 0.3 and 0.4 m. As such, the input of water from depressions to mounds is not possible. On mounds and dry locations the peat was much dryer than that in depressions. The time of filling the pit and the volume of inflowing water were smaller on mounds. The water-table depth (from the soil surface) was between 0 and − 10 cm in depressions and between −15 and −40 cm in mounds. In both settings, the first portion of supra-permafrost water that filled the pit was removed and the second portion was sampled. Sampling for CH_4 and CO_2 was performed only in wet depressions and frost cracks from the surface of flooded moss cover. GHG sampling from active layer water in mounds was not performed as digging the pit could change the gas regime. Stagnant supra-permafrost waters can be considered as oxygenated because the average O_2 saturation among all samples ranged from 3.2% to 95.5%, with an average O_2 saturation of 33 ± 20% (s.d.). There was no statistically significant difference in O_2 concentration between the 4 key sites of this study. The temperature of suprapermafrost water (SW) was similar across the latitudinal gradient: 15.4 ± 2.6 °C, 16.2 ± 6.2 °C and 17.3 ± 1.1 °C in Tazovsky, Khanymey, and Kogalym, respectively.

2.2. Analyses

Unfiltered water was sampled in 25-mL Serum bottles that were closed without air bubbles using vinyl stoppers and aluminum caps and immediately poisoned by adding 0.2 mL of saturated $HgCl_2$ using a two-way needle system. In the laboratory, a headspace was created by displacing approx. 40% of water with N_2 (99.999%). Two 0.5-mL replicates of the equilibrated headspace were analyzed for their concentrations of CH_4 and CO_2, using a Bruker GC-456 gas chromatograph (GC) equipped with flame ionization and thermal conductivity detectors. After every 10 samples, a calibration of the detectors was performed using Air Liquid gas standards (i.e., CH_4 = 145 ppmv and CO_2 = 3000 ppmv). Duplicate injection of the samples showed that results were reproducible within ±5%. The specific gas solubility for CH_4 (Yamamoto et al., 1976) and CO_2 (Weiss, 1974) were used in calculation of total CH_4 and CO_2 content in the vials and then recalculated to μmol/L of the initial waters.

Collected waters were filtered on-site in pre-washed 30-mL polypropylene Nalgene® flacons through single-use Minisart filter units (0.45 μm poresize, Sartorius, acetate cellulose filter). The first 20 mL of filtrate were discarded. Filtered solutions were divided into two parts: acidified (pH ~ 2) with ultrapure double-distilled HNO_3 for trace element analyses and non-acidified for DOC, DIC and anion analyses. Blanks were performed to control the level of contamination induced by sampling and filtration. DOC blanks of filtrate never exceeded 0.1 mg/L which is quite low for the organic-rich pore waters sampled in this study (i.e., 20–100 mg/L DOC). The UV absorbance of the filtered samples was measured at 280 nm using 10-mm quartz cuvette on a Cary-50 spectrophotometer. The specific UV-absorbency ($SUVA_{280}$, L mg^{-1} m^{-1}) was used as a proxy for aromatic C, molecular weight and source of DOM (Weishaar et al., 2003; Ilina et al., 2014 and references therein).

The pH was measured in field using a combined electrode with uncertainty of ±0.02 pH units. DOC and DIC were analyzed using a Carbon Total Analyzer (Shimadzu TOC VSCN) with an uncertainty better than 3% (see Prokushkin et al., 2011 for methodology). Major anion (Cl, SO_4) concentrations were measured by ion chromatography (HPLC, Dionex ICS 2000) with an uncertainty of 2%. International certified samples ION, PERADE, and RAIN were used for validation of analysis. Major cations (Ca, Mg, Na, K), Si, and ~40 trace elements were determined with an Agilent ce 7500 ICP-MS with In and Re as internal standards and 3 various external standards. The SLRS-5 (Riverine Water Reference Material for Trace Metals certified by the National Research Council of Canada) was used to check accuracy and reproducibility for each analysis (Yeghicheyan et al., 2013). Only those elements that exhibited good agreement between replicated measurements of SLRS-5 and the certified values (relative difference < 15%) are reported in this study. Details of trace element analyses in DOC-rich waters of western Siberia and reliability of certified samples measurements are described elsewhere (Pokrovsky et al., 2016a, 2016b).

2.3. Statistical treatment

The concentration of GHG, dissolved carbon, and major and trace elements in supra-permafrost waters at each sampling site was tested for normality, separately for each micro-landscape and for all micro landscapes at each latitude. The normality of data distribution was explored using the Shapiro-Wilk test. Because data were not normally distributed we used non-parametric statistics. Thus, the median and 1st and 3rd quartiles were used to trace dependence of element concentration from the latitude. Comparison of DOC, major and TE concentrations between supra-permafrost porewaters collected in 2 main micro landscapes (mound and hollow) and 4 sampling sites (Kogalym, Khanymey, Pangody and Tazovsky) was conducted using a non-parametric Wilcoxon-Mann Whitney test. Regressions and power functions were also used to quantify relationships between elemental concentrations and sampling latitude.

Statistical treatment of the full set of sampled supra-permafrost waters across the micro-landscapes and permafrost zones included a Principal Component Analysis (PCA) analysis using the Statistica-7 package (http://www.statsoft.com) comprising the methods for scores and variables (De la Cruz and Holmes, 2011). Principal component analysis (PCA) was used for the full set of sampled supra-permafrost waters across the micro-landscapes and permafrost zones. The PCA analysis allowed to test the influence of various parameters, notably the latitude and ALT on the supra-permafrost GHG, DOC, and elemental concentrations. All graphics and figures were created using MS Excel 2010, MS Visio Professional 2016 and GS Grapher 11 package.

3. Results

3.1. PCA and correlation between elemental concentrations

The PCA of full dataset yielded 2 possible factors contributing to observed variations in elemental concentrations (i.e., 21 and 13%, Fig. S1 of

Supplement). The first factor controlled low mobile lithogenic elements such as Al, Ga, REEs, Cr, Nb, Zr, Hf, Th and also Co, As, V, U whereas the second factor was defined by DOC and some soluble and biogenic elements such as K, Rb, Cs, Cd, Cr, Ni. Some less mobile elements (Fe, Ti and Nb) were also associated with the 2nd factor. The correlation matrix (Table S1 of Supplement) of element concentrations demonstrates a large number of elements yielding a significant ($R > 0.5$ at $p < 0.05$) and positive correlation with latitude (Mg, Al, Ca, Ti, V, Fe, Co, Ni, Ga, As, Sr, Zr, Nb, Mo, Cd, medium and heavy REE, Hf, Th). None of the major and trace elements correlated with CO_2 and CH_4 however DOC was positively correlated ($p < 0.05$) with Al ($R = 0.70$), Ti ($R = 0.77$), Cr ($R = 0.83$), Fe, Co, Ni, Cd, Hf ($0.64 \le R \le 0.77$). Al concentration significantly ($p < 0.05$) correlated ($0.76 \le R \le 0.86$) with some metals, most insoluble hydrolysates, and lithogenic elements (Ti, V, Cr, Co, Ni, Ga, Zr, Nb, all REEs, Hf and Th). It is worth noting that Fe always exhibited much lower correlation coefficients with these elements compared to Al. Lastly, Ca correlated with other alkaline-earth elements, Mn, and heavy REE, however these correlations were generally lower than those with Al. Overall Al can be considered as the best proxy for most insoluble low mobility elements. Concentrations of GHG, DOC, and divalent metal micronutrients did not correlate with any other component of the ecosystems or other dissolved element.

Methane concentration in supra-permafrost waters ranged over 1–2 orders of magnitude at each site but the median values with 1st and 3rd quartiles did not show any distinct link with latitude. No correlation of CH_4 with any dissolved component including O_2 was found across the full data set with the exception of CO_2 showing a significant link ($R = 0.71$ at $p < 0.05$) to CH_4.

3.2. Effect of micro-landscape on GHG, DOC and element concentration in test sites

The mean values with S.D. of all major and trace elements in supra-permafrost waters of three main micro-landscapes (mound, hollow and subsidence) for each region as well as the WSL-averaged values for two dominant micro-landscapes, mound and hollow, are listed in Table 2. The application of the Wilcoxon-Mann Whitney test for assessing the differences between mean values of DOC and major and trace elements in dominant micro-landscapes of each region demonstrated that a large number of elements (DOC, SO4, Ca, P, Al, Fe, Cu, Co, Zn, Mn, Pb, V, As, Sb, Mo, LREE, Th, U) depict significant differences in their concentration between different micro-landscapes (Table S2 of Supplement). The CO_2 concentration was a factor of 2.5 ± 1.0 higher in permafrost subsidences and frost cracks compared to hollows. CH_4 showed more complex behavior in these negative forms of micro-relief. In Khanymey (a region of discontinuous permafrost) CH_4 was a factor of 1.4 higher in hollows compared to subsidences however the ratio decreased to 0.59 and 0.44 in Pangody and Tazovsky (frost crack).

The minimal contrast in element concentrations between mound and hollow is observed in the most southern site (Kogalym). In Pangody (discontinuous permafrost zone), the maximal number of elements exhibited statistically different concentrations between micro-landscapes. DOC and Si were a factor of 1.5 ± 0.2 higher ($p = 0.013$ to 0.043) in mounds (or polygons) compared to hollows in all 4 sites (Fig. 2A). Al and Fe were a factor of 2.1 ± 0.4 and 1.3 ± 0.3 higher, respectively, in mounds compared to hollows (Fig. 2B). This difference was only a factor of 1.4 for Sr, 1.3 to 1.2 for Co, and 0.8 ± 0.2 for Zn. V and As were generally higher in mounds or polygons compared to hollows, or depressions or cracks. Other elements also depicted statistically significant differences in supra-permafrost water from mounds and hollows/depressions (Table S2). These are Sb (0.8 ± 0.2), Mo (0.3 to 1.4), La (1.8 to 0.3), Ba (0.8 to 1.3), Mn (0.3 to 1.8) and Pb (0.4 to 0.9), shown in Fig. 2C,D. At the same time, these elements did not show any systematic evolution of elemental ratio as a function of latitude.

3.3. Effect of latitude and permafrost zone on supra-permafrost water concentrations of DOC and metals

The first examination of the latitudinal trend of elemental concentrations in supra-permafrost waters included the Wilcoxon-Mann Whitney test for which micro-landscapes exhibited more pronounced differences between sites. Results are presented as the p-value of the difference between a given site and other sites located northward (Table S3 of the Supplement). The difference between all 4 sites tested for mounds/polygons was significant ($p < 0.05$) for DIC, Mg, K, P, Fe, Mn, Ba and U. For hollows, DOC, Co, heavy rare earth elements (HREE), Th and U exhibited significant differences between sites.

The most pronounced difference between latitude sites was observed for permafrost subsidences and frost cracks between Khanymey, Pangody and Tazovsky for DOC, DIC, Mg, Si, Al, Fe, Co, Ni, Sr, Mn, As, Cd, Li, Rb, LREE (Table S3). For hollows, the difference between 3 sites was strongly pronounced only for CO_2, Si, Fe, Co, Ni, and Mn.

The global latitudinal trend of elemental concentrations in supra-permafrost waters representing median values with 1st and 3rd quartile and minimal and maximal numbers averaged over all micro-landscapes as a function of latitude are plotted for CH_4, CO_2, DOC, $SUVA_{280\ nm}$, DIC, and pH in Fig. 3A-F. Major cations (Ca, Mg), Si, P and metals (Al, Fe) are shown in Fig. 4A-F. Other major components of supra-permafrost waters (specific conductivity, Cl^-, SO_4^{2-}, K and Na) are shown in Supplement Fig. S2. The trace elements of supra-permafrost waters that were most sensitive to the latitudinal position of sampling site are illustrated in Fig. 5A-K (Mn, Co, Ni, Cu, V, As, Sr, Mo, Li, Ga and Tl) and Fig. 6A-H (Ti, Cr, Zr, Hf, La, Ce, Th and U) whereas elements indifferent to the latitude are shown in Fig. S3A-H (Zn, Ba, Cd, Pb, Rb, Cs, Sb, and W).

The latitudinal trends were approximated by linear regression. The equations and regression coefficients (R^2) parameters for each element are listed in Table 3**.** Trends were calculated separately for two dominant micro-landscapes. Additionally, we run a general regression for all micro-landscapes simultaneously as illustrated by the solid lines with corresponding regression equation in Fig. 3–6 and Fig. S2–S3 of Supplement. Overall, 3 main patterns of concentration – latitude dependence could be distinguished:

(1) A clear trend ($R^2 > 0.5$, $p < 0.001$) of increasing concentrations northward was observed for CO_2, DOC, Mg, Ca, Si, Al, Fe, Ti, Cr, Li, Rb, V, Mn, Ni, Co, Ba, Sr, Cd, Ga, As, Zr, Nb, Mo, all REEs, Hf, Tl, Th, and U. The overall increase of concentration from sporadic/isolated to continuous permafrost zone ranged from a factor of 2 to 5, as illustrated in Figs. 3A,C,F, 4(A,B,C,E,F), 5 and 6.

(2) A lack of significant trend ($R^2 < 0.5$) of concentration with latitude was observed for CH_4, DIC, S.C., pH, SUVA, Cl, SO_4, Cs, Sb, Cu, Zn, Pb, Sb, as illustrated in Fig. 3B, E, Figs. S2 and S3 of Supplement.

(3) A decreasing concentration trend ($R^2 > 0.4$, $p < 0.05$) of P, Na, K, Pb, Sb and W was observed and is shown in Fig. 4D, Figs. S2 E, D; S3 D, G, and H, respectively.

3.4. Comparison of elemental concentration and latitudinal trends between supra-permafrost waters, lakes, and rivers of permafrost-affected zones in the WSL

Chemical composition of supra-permafrost waters and their latitudinal trend can be compared with those of major and trace elements in thermokarst (thaw) lakes of western Siberia. These lakes are shallow (0.5–1.5 m depth) water bodies that are widely distributed north of 62°N where they may occupy 30 to 80% of the watershed area (Pokrovsky et al., 2014; Polishchuk et al., 2017, 2018). The average concentrations of major and TE in thermokarst lakes of various sizes across a latitudinal gradient from 63°N to 67°N (Manasypov et al., 2014) can be compared with average concentrations of major and TE in supra-permafrost waters collected in this study. For this plot, summer-period

Table 2
Mean values with s.d. of elements in suprapermafrost waters across the permafrost gradient of western Siberia Lowland. The DOC, DIC, Cl, SO_4, Si, Ca, Mg, Na, K, P, Al, and Fe concentrations are in mg/L and all other trace element are in μg/L.

Component	Kogalym (62.259°N)		Khanymey (63.785°N)			Pangody (65.873°N)			Tazovsky (67.357°N)			WSL-mean mound/ poligon	WSL mean hollow
	Mound $n = 6$	Hollow n = 6	Mound $n = 16$	Hollow $n = 5$	Subsidence n = 10	Mound $n = 9$	Hollow $n = 10$	Subsidence n = 9	Poligon n = 9	Hollow n = 10	Frost crack $n = 11$		
CH_4	–	13.3 ± 26	–	4.13 ± 2.7	3.03 ± 3.1	–	10.2 ± 6.25	17.4 ± 20.34	–	3.69 ± 3.74	8.38 ± 11.6	–	8.51
CO_2	–	423 ± 399	–	192 ± 107	514 ± 205	–	562 ± 214	770 ± 629	–	471 ± 45	942 ± 488	–	447
pH	3.7 ± 0.3	3.7 ± 0.2	3.2 ± 0.2	3.7 ± 0.2	3.5 ± 0.3	3.9 ± 0.2	3.9 ± 0.1	3.8 ± 0.1	4.7 ± 0.5	4.4 ± 0.6	3.88 ± 0.15	3.8	4.04
Cond	76.5 ± 27.1	52.5 ± 13.8	90.7 ± 15.1	67 ± 14.5	68.9 ± 11.7	71.1 ± 19.2	51.9 ± 18.7	62 ± 11.9	53 ± 8	47 ± 12	68.5 ± 19.4	76.1	52.5
DOC	66.6 ± 23.9	36.9 ± 11.41	81.9 ± 22.0	51 ± 3.45	62.3 ± 11.63	107.1 ± 36.2	60.57 ± 39.0	80.9 ± 15.6	82.21 ± 16.71	58.7 ± 24.8	95.9 ± 36.8	85.9	53.9
DIC	1.24 ± 0.10	1.43 ± 0.20	1.72 ± 0.28	2.13 ± 1.07	1.8 ± 0.41	1.76 ± 0.26	1.88 ± 0.72	1.73 ± 0.23	1.91 ± 1.31	1.7 ± 0.6	1.44 ± 0.16	1.72	1.77
Cl^-	0.60 ± 0.41	0.44 ± 0.24	0.36 ± 0.24	0.21 ± 0.08	0.23 ± 0.06	0.2 ± 0.08	0.27 ± 0.27	0.18 ± 0.18	0.42 ± 0.41	0.42 ± 0.34	0.53 ± 0.35	0.53	1.01
SO_4^{2-}	0.12 ± 0.05	0.23 ± 0.19	0.59 ± 0.49	0.11 ± 0.08	0.07 ± 0.06	0.25 ± 0.3	0.08 ± 0.03	0.04 ± 0.04	0.66 ± 0.73	0.26 ± 0.21	0.46 ± 0.46	0.52	0.21
Ca	0.44 ± 0.23	0.72 ± 0.20	0.60 ± 0.26	0.68 ± 0.26	0.88 ± 0.4	1.02 ± 0.37	0.72 ± 0.34	1.21 ± 0.54	5.04 ± 2.33	3.31 ± 1.67	4.10 ± 1.52	1.66	1.52
Mg	0.18 ± 0.05	0.14 ± 0.06	0.11 ± 0.04	0.15 ± 0.05	0.12 ± 0.04	0.45 ± 0.3	0.31 ± 0.14	0.49 ± 0.25	0.69 ± 0.6	0.65 ± 0.30	0.55 ± 0.37	0.32	0.36
K	0.60 ± 0.30	0.44 ± 0.24	0.31 ± 0.17	0.62 ± 0.69	0.39 ± 0.32	0.32 ± 0.27	0.33 ± 0.21	0.34 ± 0.19	0.26 ± 0.21	0.22 ± 0.11	0.59 ± 0.4	0.33	0.36
P	0.41 ± 0.16	0.23 ± 0.06	0.24 ± 0.11	0.22 ± 0.2	0.21 ± 0.14	0.2 ± 0.12	0.17 ± 0.09	0.17 ± 0.1	0.17 ± 0.11	0.19 ± 0.15	0.23 ± 0.11	0.23	0.20
Al	0.23 ± 0.07	0.09 ± 0.04	0.25 ± 0.16	0.39 ± 0.18	0.25 ± 0.08	0.74 ± 0.71	0.26 ± 0.18	0.44 ± 0.3	0.78 ± 0.28	0.47 ± 0.27	0.61 ± 0.2	0.48	0.31
Fe	0.78 ± 0.44	0.48 ± 0.24	0.34 ± 0.17	0.61 ± 0.38	0.54 ± 0.22	2.20 ± 1.27	1.45 ± 0.80	2.17 ± 1.46	1.56 ± 1.29	1.63 ± 0.93	1.73 ± 0.96	1.07	1.19
Si	1.67 ± 0.81	1.19 ± 0.71	1.64 ± 0.96	0.96 ± 0.64	0.95 ± 0.33	3.63 ± 2.17	2.05 ± 0.76	2.72 ± 1.76	3.80 ± 2.32	3.0 ± 2.03	2.89 ± 0.98	2.56	2.02
Li	0.43 ± 0.14	0.43 ± 0.14	0.52 ± 0.21	0.56 ± 0.10	0.55 ± 0.1	1.11 ± 0.64	0.69 ± 0.29	1.1 ± 0.64	0.78 ± 0.31	1.33 ± 1.19	0.90 ± 0.46	0.66	0.76
B	–	–	3.54 ± 2.83	2.16 ± 1.24	3.21 ± 2.36	1.92 ± 1.17	3.22 ± 3.15	3.04 ± 2.93	4.81 ± 3.73	2.91 ± 1.86	4.29 ± 2.96	3.04	2.36
Na	0.32 ± 0.13	0.41 ± 0.32	0.29 ± 0.17	0.33 ± 0.10	0.29 ± 0.15	0.35 ± 0.21	0.24 ± 0.16	0.24 ± 0.10	0.2 ± 0.13	0.27 ± 0.21	0.24 ± 0.13	0.29	0.30
Ti	1.71 ± 0.62	1.06 ± 0.42	2.89 ± 1.6	3.07 ± 1.49	2.41 ± 1.34	4.59 ± 1.66	2.11 ± 1.59	4.1 ± 3.50	3.93 ± 1.46	3.69 ± 2.25	4.25 ± 1.6	3.37	2.52
V	0.569 ± 0.47	0.19 ± 0.088	0.48 ± 0.46	0.65 ± 0.45	0.5 ± 0.49	0.79 ± 0.44	0.26 ± 0.23	0.43 ± 0.37	5.09 ± 2.9	2.72 ± 2.68	2.39 ± 1.15	1.58	1.06
Cr	1.19 ± 0.47	0.80 ± 0.24	1.07 ± 0.49	1.12 ± 0.22	1.1 ± 0.39	1.67 ± 1.65	1.24 ± 0.49	1.61 ± 0.55	1.79 ± 0.42	1.26 ± 0.63	2.14 ± 0.94	1.38	1.14
Mn	3.71 ± 1.11	5.59 ± 2.93	1.91 ± 1.93	5.77 ± 3.20	3.55 ± 2.84	20.08 ± 10.7	10.53 ± 8.47	16.6 ± 13.24	208.5 ± 89.1	0.14 ± 0.08	108.3 ± 87.3	52.05	47.99
Co	0.15 ± 0.03	0.11 ± 0.07	0.15 ± 0.07	0.27 ± 0.12	0.21 ± 0.09	1.78 ± 0.82	0.97 ± 0.61	1.5 ± 0.97	2.09 ± 1.17	1.74 ± 0.79	2.02 ± 0.92	0.94	0.94
Ga	0.04 ± 0.03	0.03 ± 0.01	0.05 ± 0.029	0.07 ± 0.04	0.04 ± 0.026	0.08 ± 0.07	0.05 ± 0.04	0.052 ± 0.013	0.06 ± 0.02	0.07 ± 0.02	0.07 ± 0.02	0.057	0.055
As	0.77 ± 0.29	0.74 ± 0.16	0.53 ± 0.16	0.7 ± 0.18	0.52 ± 0.1	1.72 ± 1.73	0.73 ± 0.40	0.9 ± 0.43	4.11 ± 3.47	1.79 ± 1.16	1.84 ± 0.87	1.62	1.06
Rb	0.77 ± 0.27	0.55 ± 0.27	0.72 ± 0.47	0.55 ± 0.47	0.58 ± 0.26	1.31 ± 0.85	0.70 ± 0.57	1.08 ± 0.74	0.68 ± 0.28	0.78 ± 0.60	2.23 ± 1.99	0.85	0.67
Zr	0.058 ± 0.037	0.055 ± 0.02	0.146 ± 0.132	0.19 ± 0.11	0.11 ± 0.08	0.43 ± 0.25	0.32 ± 0.25	0.429 ± 0.404	1.31 ± 0.55	0.71 ± 0.35	1.03 ± 0.74	0.457	0.368
Nb	0.017 ± 0.011	0.012 ± 0.007	0.029 ± 0.02	0.036 ± 0.008	0.022 ± 0.006	0.068 ± 0.042	0.040 ± 0.023	0.074 ± 0.059	0.067 ± 0.018	0.047 ± 0.03	0.08 ± 0.05	0.045	0.036
Mo	0.011 ± 0.003	0.035 ± 0.06	0.033 ± 0.029	0.038 ± 0.034	0.033 ± 0.029	0.052 ± 0.041	0.030 ± 0.038	0.027 ± 0.011	0.091 ± 0.045	0.069 ± 0.03	0.09 ± 0.03	0.048	0.044
Cd	0.033 ± 0.014	0.051 ± 0.019	0.068 ± 0.054	0.092 ± 0.082	0.05 ± 0.019	0.054 ± 0.027	0.052 ± 0.024	0.083 ± 0.036	0.068 ± 0.03	0.063 ± 0.05	0.124 ± 0.07	0.064	0.061
Ni	0.54 ± 0.09	0.75 ± 0.39	0.62 ± 0.24	1.22 ± 0.66	0.77 ± 0.3	3.97 ± 2.11	2.46 ± 1.46	3.04 ± 1.76	5.10 ± 1.09	3.48 ± 1.02	6.09 ± 3.36	2.35	2.25
Cu	0.71 ± 0.23	1.48 ± 0.61	0.52 ± 0.46	0.7 ± 0.07	0.52 ± 0.32	0.74 ± 0.63	0.84 ± 0.83	1.18 ± 1.03	3.49 ± 2.30	1.39 ± 0.69	3.36 ± 2.31	1.25	1.12
Zn	8.92 ± 4.04	11.40 ± 2.55	9.04 ± 4.58	11.74 ± 4.19	11.63 ± 4.61	5.02 ± 2.17	8.11 ± 4.53	13.75 ± 5.75	7.10 ± 6.37	9.38 ± 4.25	19.29 ± 10.4	7.70	9.69
Sr	6.54 ± 2.96	4.35 ± 1.79	4.63 ± 1.71	6.21 ± 2.8	6.43 ± 2.39	14.13 ± 3.87	9.39 ± 6.72	12.85 ± 5.46	26.7 ± 8.2	17.53 ± 9.21	21.71 ± 6.73	11.87	10.44
Sb	0.055 ± 0.026	0.08 ± 0.03	0.035 ± 0.011	0.05 ± 0.01	0.04 ± 0.01	0.028 ± 0.02	0.05 ± 0.01	0.06 ± 0.014	0.04 ± 0.01	0.04 ± 0.012	0.05 ± 0.017	0.037	0.056

(continued on next page)

Table 2 (*continued*)

Component	Kogalym (62.259°N)		Khanymey (63.785°N)			Pangody (65.873°N)			Tazovsky (67.357°N)			WSL-mean mound/ poligon	WSL mean hollow
	Mound $n = 6$	Hollow n = 6	Mound $n = 16$	Hollow $n = 5$	Subsidence n = 10	Mound $n = 9$	Hollow $n = 10$	Subsidence n = 9	Poligon n = 9	Hollow n = 10	Frost crack $n = 11$		
Cs	0.031 ± 0.004	0.021 ± 0.008	0.050 ± 0.032	0.03 ± 0.022	0.039 ± 0.02	0.03 ± 0.018	0.023 ± 0.023	0.026 ± 0.03	0.023 ± 0.01	0.012 ± 0.01	0.08 ± 0.075	0.037	0.020
Ba	12.5 ± 1.2	15.2 ± 3.1	15.8 ± 1.9	15.4 ± 3.5	17.8 ± 3.9	25.13 ± 11.55	18.44 ± 6.97	20.2 ± 5	18.28 ± 5.99	17.96 ± 9.16	22.83 ± 7.11	18.1	17.2
La	0.074 ± 0.029	0.048 ± 0.03	0.08 ± 0.07	0.20 ± 0.14	0.11 ± 0.12	0.132 ± 0.049	0.1 ± 0.08	0.227 ± 0.21	0.75 ± 0.37	0.35 ± 0.25	0.35 ± 0.21	0.242	0.181
Ce	0.166 ± 0.067	0.094 ± 0.05	0.19 ± 0.15	0.43 ± 0.30	0.23 ± 0.27	0.609 ± 0.604	0.27 ± 0.21	0.3 ± 0.296	1.73 ± 0.86	0.88 ± 0.58	0.86 ± 0.54	0.621	0.446
Pr	0.020 ± 0.008	0.011 ± 0.005	0.022 ± 0.018	0.05 ± 0.03	0.024 ± 0.03	0.054 ± 0.02	0.03 ± 0.02	0.021 ± 0.009	0.23 ± 0.11	0.12 ± 0.08	0.12 ± 0.078	0.075	0.056
Nd	0.080 ± 0.032	0.041 ± 0.022	0.089 ± 0.076	0.19 ± 0.12	0.10 ± 0.12	0.141 ± 0.105	0.141 ± 0.11	0.127 ± 0.134	0.99 ± 0.48	0.51 ± 0.33	0.53 ± 0.34	0.299	0.242
Sm	0.017 ± 0.007	0.0094 ± 0.005	0.019 ± 0.016	0.040 ± 0.027	0.022 ± 0.023	0.031 ± 0.02	0.026 ± 0.018	0.02 ± 0.006	0.224 ± 0.11	0.119 ± 0.08	0.12 ± 0.076	0.067	0.053
Eu	0.005 ± 0.001	0.0034 ± 0.0012	0.005 ± 0.002	0.009 ± 0.005	0.006 ± 0.005	0.013 ± 0.014	0.008 ± 0.005	0.0052 ± 0.002	0.055 ± 0.027	0.029 ± 0.02	0.03 ± 0.018	0.018	0.014
Gd	0.018 ± 0.008	0.012 ± 0.0055	0.019 ± 0.016	0.038 ± 0.023	0.021 ± 0.021	0.032 ± 0.021	0.026 ± 0.017	0.019 ± 0.010	0.241 ± 0.119	0.128 ± 0.08	0.13 ± 0.081	0.071	0.056
Tb	0.0025 ± 0.0009	0.001 ± 0.0005	0.003 ± 0.002	0.006 ± 0.003	0.003 ± 0.003	0.005 ± 0.002	0.005 ± 0.002	0.003 ± 0.001	0.035 ± 0.02	0.02 ± 0.01	0.02 ± 0.011	0.010	0.008
Dy	0.014 ± 0.005	0.008 ± 0.004	0.016 ± 0.014	0.03 ± 0.016	0.016 ± 0.017	0.023 ± 0.014	0.021 ± 0.015	0.014 ± 0.006	0.205 ± 0.09	0.11 ± 0.07	0.113 ± 0.07	0.059	0.046
Ho	0.0024 ± 0.0008	0.002 ± 0.0007	0.003 ± 0.003	0.006 ± 0.003	0.003 ± 0.003	0.005 ± 0.002	0.004 ± 0.003	0.003 ± 0.001	0.04 ± 0.02	0.022 ± 0.01	0.02 ± 0.014	0.012	0.009
Er	0.0060 ± 0.0019	0.0041 ± 0.0014	0.009 ± 0.007	0.016 ± 0.008	0.009 ± 0.008	0.022 ± 0.02	0.012 ± 0.009	0.009 ± 0.004	0.123 ± 0.058	0.067 ± 0.04	0.07 ± 0.046	0.037	0.028
Tm	0.0009 ± 0.0003	0.0008 ± 0.0004	0.0012 ± 0.001	0.002 ± 0.001	0.001 ± 0.001	0.004 ± 0.003	0.002 ± 0.001	0.002 ± 0.0024	0.018 ± 0.008	0.010 ± 0.01	0.01 ± 0.006	0.005	0.004
Yb	0.0051 ± 0.0022	0.0037 ± 0.0018	0.008 ± 0.006	0.013 ± 0.006	0.008 ± 0.006	0.017 ± 0.01	0.022 ± 0.024	0.013 ± 0.017	0.121 ± 0.057	0.067 ± 0.04	0.07 ± 0.043	0.035	0.031
Lu	0.0008 ± 0.0003	0.0007 ± 0.0004	0.0012 ± 0.001	0.002 ± 0.001	0.001 ± 0.0009	0.003 ± 0.001	0.0016 ± 0.001	0.002 ± 0.002	0.019 ± 0.009	0.011 ± 0.01	0.01 ± 0.006	0.005	0.004
Hf	0.0067 ± 0.0053	0.0052 ± 0.0023	0.009 ± 0.008	0.011 ± 0.003	0.006 ± 0.002	0.029 ± 0.02	0.023 ± 0.019	0.043 ± 0.041	0.090 ± 0.037	0.048 ± 0.04	0.07 ± 0.052	0.031	0.025
W	0.015 ± 0.002	0.019 ± 0.009	0.01 ± 0.009	0.013 ± 0.009	0.013 ± 0.019	0.009 ± 0.005	0.013 ± 0.01	0.009 ± 0.005	0.007 ± 0.003	0.01 ± 0.004	0.01 ± 0.003	0.010	0.013
Tl	0.0016 ± 0.0013	0.0025 ± 0.002	0.004 ± 0.003	0.004 ± 0.003	0.005 ± 0.004	0.007 ± 0.006	0.003 ± 0.002	0.004 ± 0.002	0.01 ± 0.008	0.006 ± 0.01	0.013 ± 0.01	0.006	0.004
Pb	0.40 ± 0.20	0.79 ± 0.26	0.59 ± 0.48	1.06 ± 0.58	0.83 ± 0.51	0.379 ± 0.203	0.80 ± 0.54	0.68 ± 0.39	0.358 ± 0.176	0.45 ± 0.28	0.91 ± 0.484	0.47	0.73
Th	0.012 ± 0.007	0.007 ± 0.004	0.020 ± 0.012	0.047 ± 0.047	0.026 ± 0.031	0.052 ± 0.048	0.030 ± 0.021	0.05 ± 0.06	0.114 ± 0.063	0.06 ± 0.03	0.08 ± 0.056	0.047	0.037
U	0.0026 ± 0.0016	0.0025 ± 0.001	0.011 ± 0.01	0.014 ± 0.015	0.012 ± 0.012	0.014 ± 0.011	0.012 ± 0.016	0.012 ± 0.011	0.034 ± 0.02	0.021 ± 0.02	0.015 ± 0.01	0.016	0.013

concentrations of lakes smaller than 500,000 m^2 can be used since the feeding of thermokarst lakes by supra-permafrost influx is maximal in August during highest active layer thickness (Manasypov et al., 2014). Larger lakes were not used for this comparison because they may have groundwater feeds and surface water inlets (Manasypov et al., 2015). The concentrations of elements in lakes are different from concentrations in supra-permafrost waters yet the latitudinal trends are generally reproduced for many elements as shown by dashed lines in Figs. 7 and S4 of Supplement. Concentrations of DOC, Si, Fe, Al, and Pb in lakes are always a factor of 2 to 10 lower than those in supra-permafrost waters. Simultaneously, within the permafrost zone, concentrations of K, Cu, Ti, Ni, Mo, Sb, As, Cr, Zn, Cd, V and U in lake waters are comparable (within scatter of data points) to those in supra-permafrost waters.

The comparison of supra-permafrost waters with river waters was performed for rivers whose watershed was smaller than 10,000 km^2 as larger rivers may have significant underground feeding via taliks under the river beds (i.e., Baulin et al., 1967; Romanovsky, 1983; Fotiev, 1989, 1991; Ivanov and Beshentsev, 2005). The summer-time elemental concentrations in rivers located between 63 and 68°N shown by dotted lines in Figs. 7 and S4 demonstrated a similar trend of increasing concentration northwards of 64°N for Ca, Mg, Sr, Ni, Mo, and U. The concentration patterns of K, Rb, Zn, Cd and Pb in both soil waters and rivers were independent of latitude. Finally, the northward increase of Fe, Al, Si, DOC, CO_2 in supra-permafrost waters was not consistent with the pattern of these elements in rivers. The concentrations of DIC, Ca, Mg, Si, Sr in rivers were a factor of 2 to 10 higher than those in supra-permafrost waters; alternatively, DOC, Fe, Al, Ti, Ga, Zr, Hf, Th, Pb, and Cd in supra-permafrost waters strongly exceeded levels in rivers.

4. Discussion

4.1. Organic carbon in peat soil waters and GHG emission potential across permafrost zones

A northward increase (as opposed to decrease) of DOC and CO_2 concentrations in supra-permafrost waters of WSL is somehow counterintuitive given that the colder climate and lower ALT and biomass should act against such an increase in northern continuous to discontinuous permafrost sites relative to southern sporadic to isolated sites. At present, in a larger latitudinal gradient comprising both southern (permafrost-free) and northern part of WSL (53°N to 68°N), two main hypotheses were suggested to explain elevated DOC concentrations and fluxes in permafrost-affected rivers relative to permafrost-free rivers. The first possible explanation comes from a study of the Yenisey River

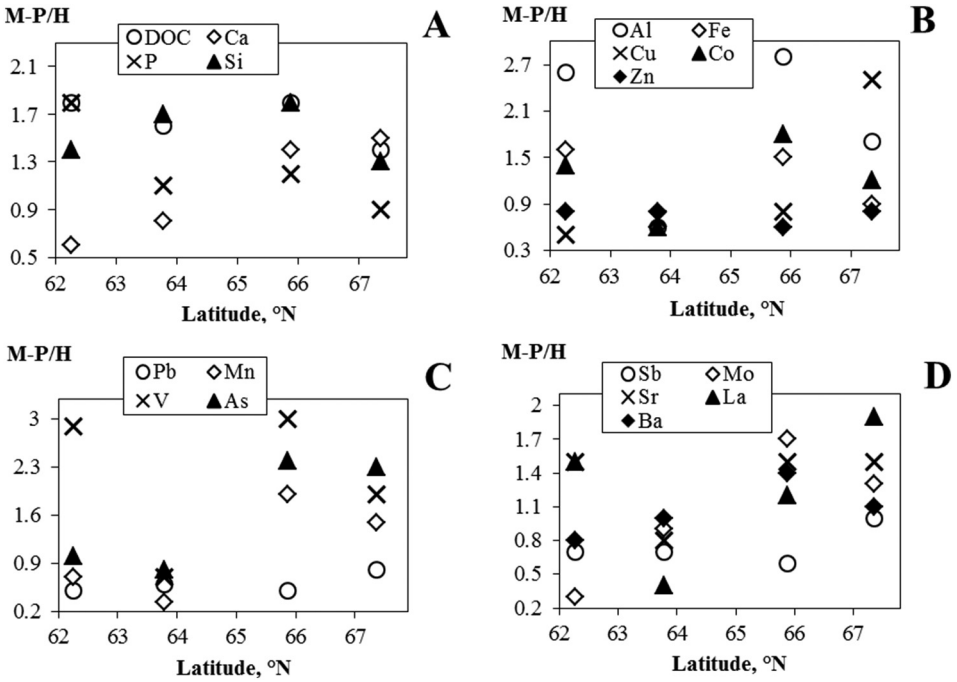

Fig. 2. The ratio of elemental concentrations in supra-permafrost waters collected from positive forms of micro-relief (peat mound – M, polygons – P) to that in negative forms (hollows – H) across the WSL permafrost zone. The ratios of mean values from Table 2 were used to draw plots.

Basin which revealed that the dissolved organic matter (DOM) in northern permafrost-affected tributaries was significantly less biodegradable than that in southern tributaries, thus producing an enrichment in northern streams of soil DOM (Kawahigashi et al., 2004). It is therefore possible that the DOM of supra-permafrost water in continuous and discontinuous permafrost zone (sites Pangody, Tazovsky) is better preserved because it is less biodegradable than DOM of supra-permafrost water in sporadic to isolated regions (site Kogalym). However, optical properties of DOM cannot confirm this hypothesis as the $SUVA_{280}$ remained highly constant across the latitudinal/permafrost gradient and ranged from 2.7 to 3.5 L mg^{-1} m^{-1} in all sites (Fig. 3 D) which is consistent with values in lakes (2 to 4 L mg^{-1} m^{-1}, Manasypov et al., 2015) and rivers (2 to 3.5 L mg^{-1} m^{-1}, Pokrovsky et al., 2015) of the region during the summer period. Given that the SUVA is not a straightforward measure of biodegradability, molecular-size characterization and bioassays of DOM (cf., Roehm et al., 2009) in WSL soil solutions are necessary. Another argument against poorer biodegradability of DOC in northern sites relative to southern sites is the 1.5 to 2 times higher concentration of CO_2 in supra-permafrost waters of the Tazovsky and Pangody regions compared to Kogalym and Khanymey regions (Fig. 3A). This difference (significant at $0.003 \le p \le 0.042$ of Wilcoxon-Mann Whitney test) indirectly suggests more intensive bacterial respiration of soil DOM in northern sites.

The second possible explanation for elevated DOC concentrations in northern soil waters relative to southern soil waters is that the DOC can be retained by clay horizons in permafrost-poor sites whereas in permafrost–bearing sites the supra-permafrost flow occurs exclusively within the organic layer (see Smedberg et al., 2006 for discussion). Such a mechanism has been hypothesized to be the main driver of DOC gradient in rivers within a large latitudinal transect of WSL from permafrost-free to continuous permafrost zones (Pokrovsky et al., 2015). The latter authors reported the 2 to 3 times higher DOC export fluxes from river watersheds located at 67.5°N relative to those at 64°N.

Because the DOC in soil waters originates from leaching of peat and plant litter we suggest, in accord with earlier observations on rivers (Carey, 2003), that the DOC export from the permafrost – affected watersheds is controlled by DOC residence time and travel pathway through the organic topsoil. Thus, a recent study of DOC fluxes in the Qinghai-Tibetan Plateau over a gradient of ALT demonstrated that a gradual active layer deepening may decrease DOC export from the permafrost catchments (Mu et al., 2017). Generally, the active layer water is recharged by warm season rainfall but is also supplied by the seasonal ice melt of active layer (Throckmorton et al., 2016). The supra-permafrost waters in the continuous permafrost zone remain for long periods of time in a frozen state and thus, during the warm season, are replaced to a lesser degree by snowmelt and rain water as compared to waters from discontinuous to sporadic permafrost zones (Novikov et al., 2009). Because this replacement requires more time in the north, the active layer waters in continuous permafrost zones exhibit the longest residence time in the peat profile. The hydrological connectivity of frozen palsa peat bogs to surrounding streams and temporary water channels is also lower in the north than in the south (Novikov et al., 2009). Therefore, the northern regions offer longer contact between peat layers and vertically infiltrating and laterally migrating water whereas in south of the permafrost zone, the active layer water transfers from intra-peat to surface runoff quite fast.

Additional evidence of the stronger enrichment in DOC of supra-permafrost waters in the north comes from peat porosity. Thus, the leaching of peat constituents by downward penetrating and laterally moving fluids may be more efficient in the north due to more condensed and less porous peat which imposes greater residence time of soil fluids. Studies of physical properties on peat in the WSL demonstrated that the porosity coefficient of peat decreases with the increase in degree of decomposition (Kramarenko and Emel'yanova, 2009). The peat in the north of the WSL (continuous to discontinuous permafrost zones) has a higher degree of decomposition compared to southern regions such as Kogalym (Liss et al., 2001) and can have lower porosity yielding higher residence time for supra-permafrost waters. Gravimetric water content in WSL peatlands which ranges from 92 to 89% in non-permafrost sites and from 81 to 85% in permafrost sites is consistent with this (Smith et al., 2012). An additional factor for decreasing the supra-permafrost water residence time in peat in southern regions is the doubled precipitation level in comparison to northern regions (594 mm in Kogalym and 363 mm in Tazovsky, see Table 1). Intensive wash-out regime of the upper peat horizons may lead to sizably lower concentrations of DOC and other solutes in SW of southern sites.

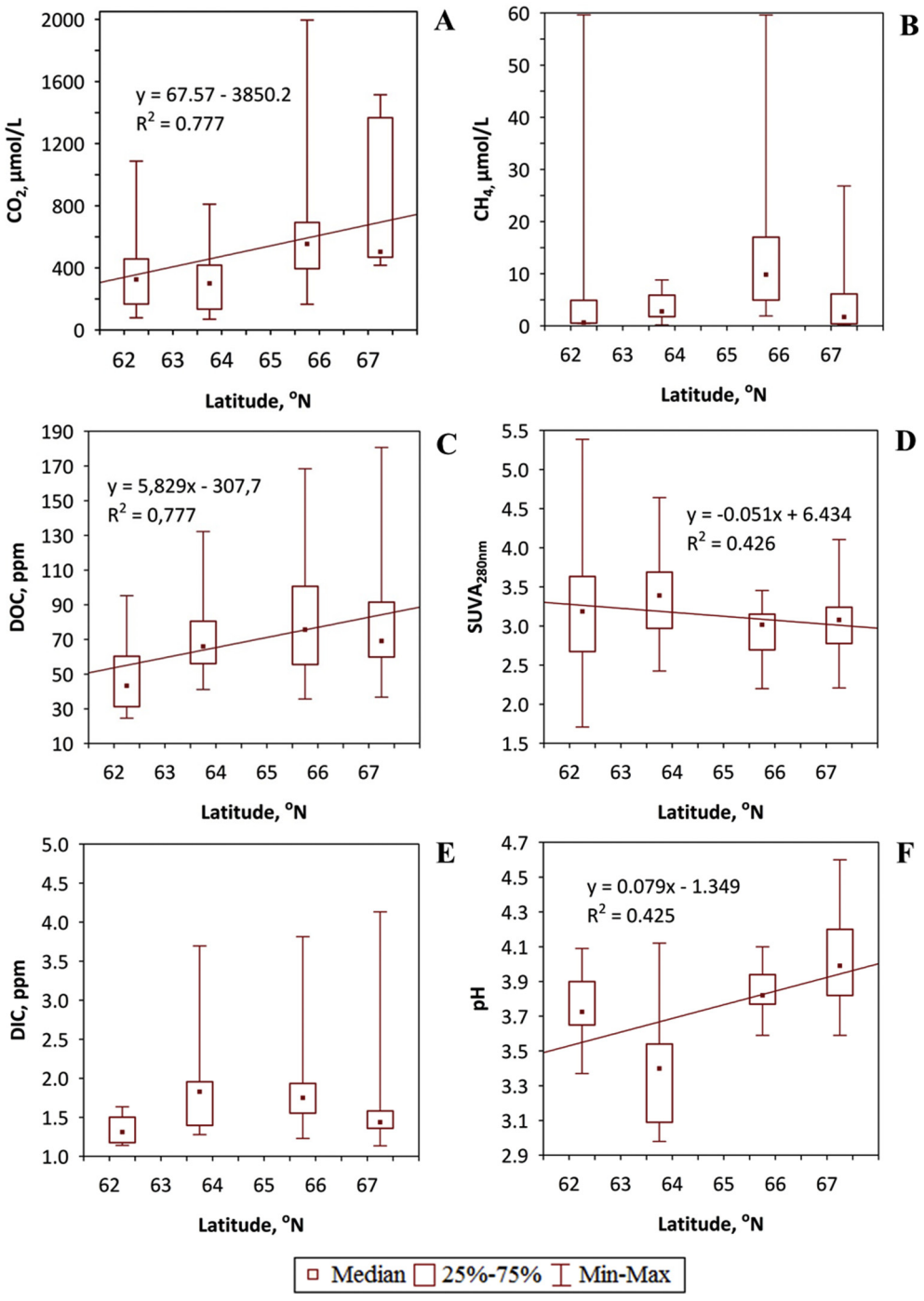

Fig. 3. A-F. The general latitudinal trend in CO_2 (**A**), CH_4 (**B**), DOC (**C**), SUVA (**D**), DIC (**E**) concentrations and pH (**F**) together with mean values over all micro-landscapes treated together. The individual linear regressions for each micro-landscape are listed in Table 3.

Taken together, the local hydrological pathway within the peat pores can essentially control the overall enrichment of supra-permafrost waters through dissolved organic matter from the peat constituents. Note that there is no contradiction with well-established fact that deep flow paths could decrease DOC export, since DOC mineralization and adsorption are higher when water spends more time in soil prior to reaching the stream network (Koch et al., 2013; Tetzlaff et al., 2015; Ma et al., 2017). In the latter studies, the active layer fluids travel through the mineral soil, which are capable to remove and fractionate DOM via adsorption and retention.

The CO_2 and CH_4 emission potential of supra-permafrost waters can be estimated from GHG concentration patterns across the WSL (Fig. 3A, B). Both CO_2 and CH_4 concentrations of supra-permafrost waters are at the upper limit of their concentrations (>100 and >1 μmol/L, respectively) that were reported in small (<10 m^2) depressions in discontinuous permafrost zones (Shirokova et al., 2013; Polishchuk et al., 2018). These depressions are usually fed by supra-permafrost waters (Pokrovsky et al., 2016b; Loiko et al., 2017). Given a strong supersaturation of supra-permafrost waters with respect to atmospheric CO_2 and CH_4, the GHG emission potential of shallow subsurface waters present in the WSL frozen peat province is quite high, especially in the northern continuous permafrost-affected zones. In fact, there is a strongly pronounced northward increasing trend of CO_2 concentration with latitude in supra-permafrost waters from subsidences/frost cracks ($R^2 = 0.996$,

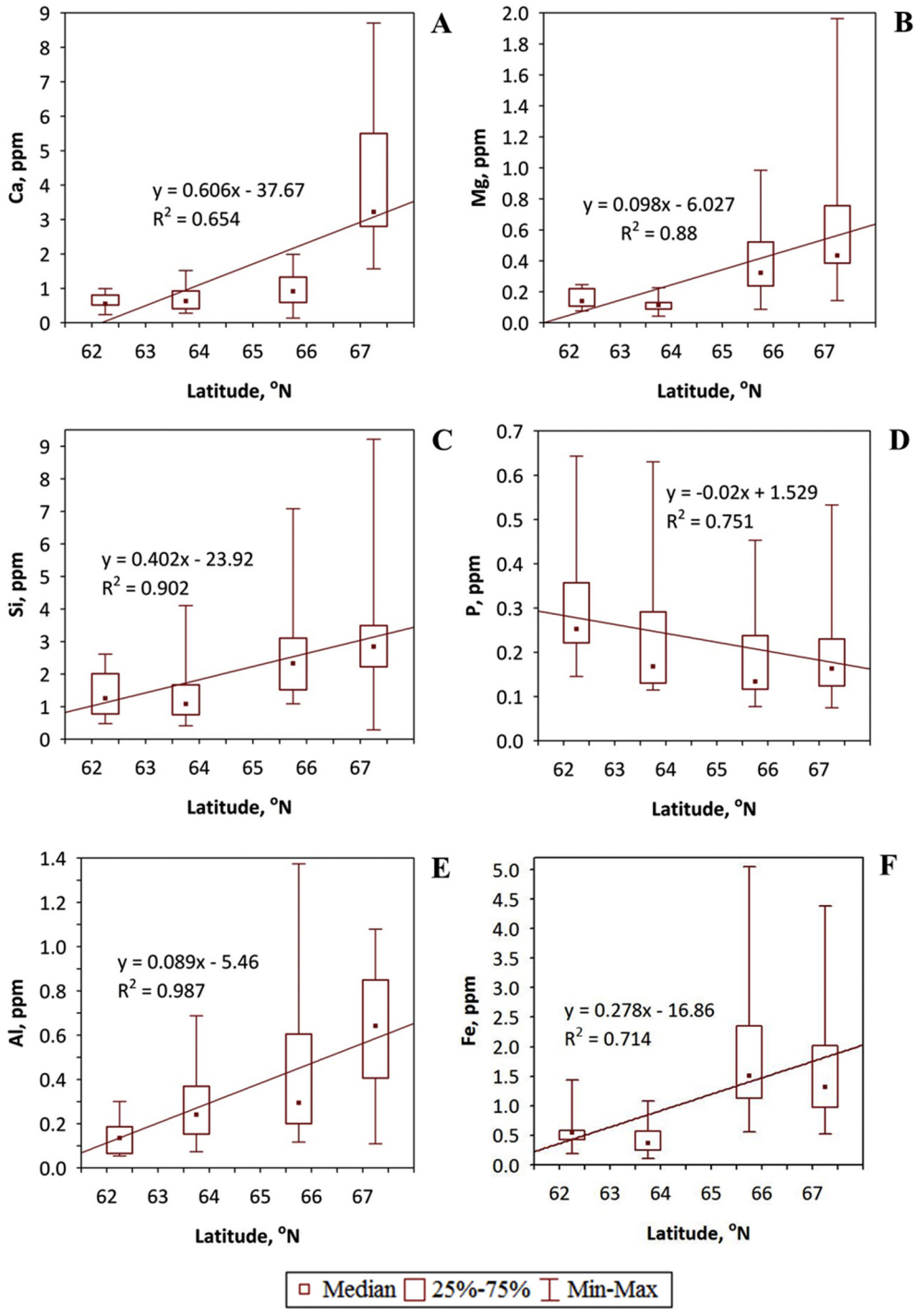

Fig. 4. The general latitudinal trend in Ca (**A**), Mg (**B**), Si (**C**), P (**D**), Al (**E**) and Fe (**F**) concentration (mg/L) over all micro-landscapes treated together using linear regressions as a function of latitude. The individual linear regressions for each micro-landscape are listed in Table 3.

Table 3). The CO_2 concentration in the polygonal tundra of the Tazovsky site is roughly 2 times higher than that in discontinuous permafrost zone of the Khanymey's palsa. At present, quantification of the proportion of free soil water over large areas of the WSL is necessary to upscale current observations for the emission flux from stagnant surface and soil waters to the atmosphere.

4.2. Factors controlling major and trace element concentration in supra-permafrost peat soil solution of the WSL

An unexpected result of this study was that most major and trace elements (notably Ca, Mg, Si, Fe, Al) increased their concentration in supra-permafrost waters northward, by a factor of 2 to 5 between sporadic and continuous permafrost zones, and only Na, K, Cs, P, Sb, and W yielded a sizeable decrease in concentration northward. This is contradictory to the general understanding of the WSL geographical setting and knowledge of chemical weathering in boreal and subarctic zones. In the WSL, the following factors should decrease supra-permafrost water element concentrations northward: *i*) a decrease in the thickness of the active soil (peat) layer leading to the decrease of the amount of peat interacting with downward penetrating fluids; *ii*) a decrease in plant biomass (Frey and Smith, 2007) and related plant ability to weather minerals within the soil profile; *iii*) a shortening of the unfrozen period of the year. However, these factors were presumably not capable

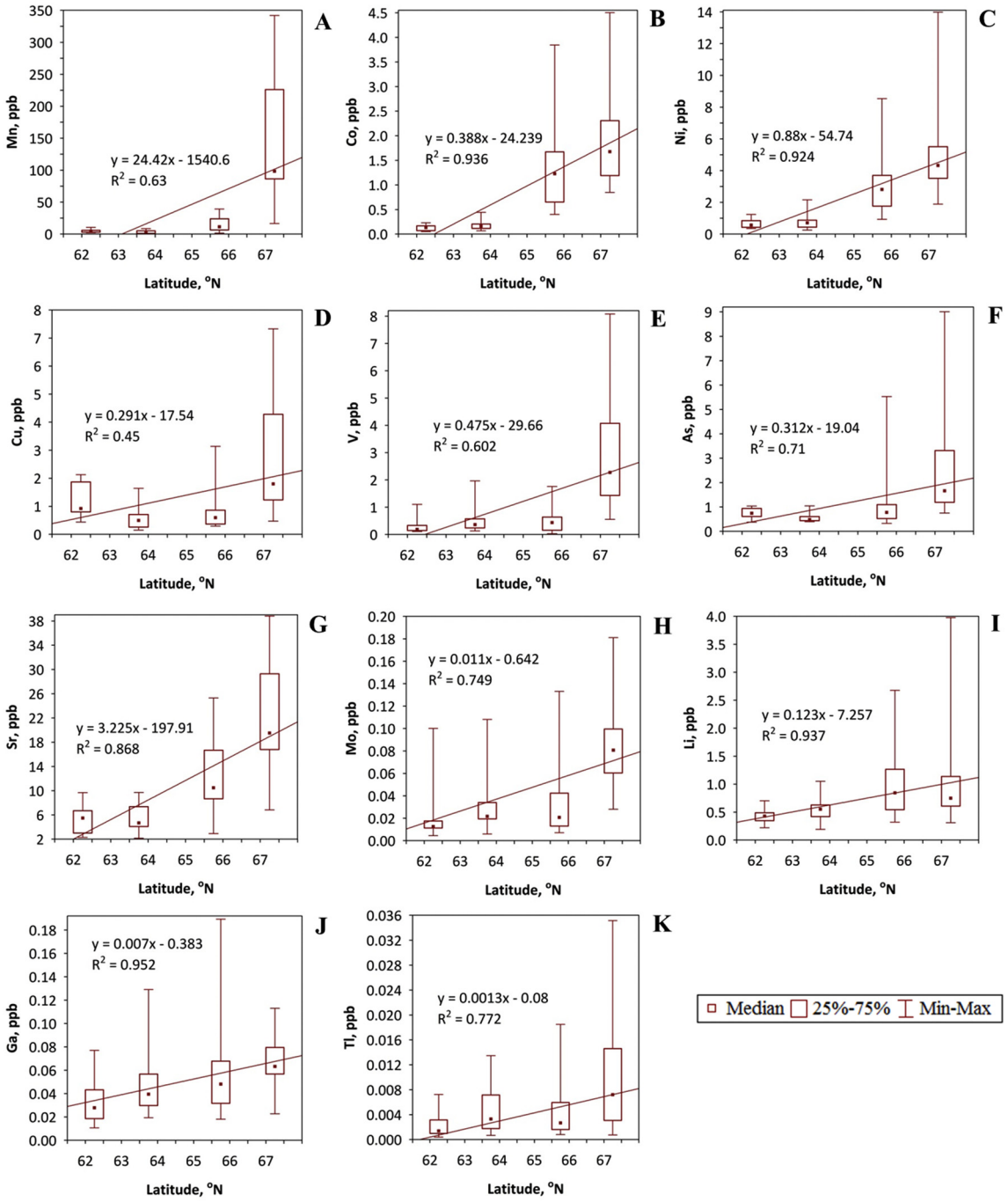

Fig. 5. Trace element (Mn, Co, Ni, Cu, V, As, Sr, Mo, Li, Ga, and Tl) concentration (μg/L) in suprapermafrost waters of the WSL as a function of latitude. The solid lines are linear regressions run over all micro-landscapes.

decreasing element concentrations northwards. Note here that the marine aerosol deposition on the supra-permafrost water chemistry can be dismissed because Na, Cl, and SO_4 concentrations are not significantly ($p < 0.05$) higher and are even lower in coastal regions (Tazovsky) compared to continental sites (Pangody, Khanymey, and Kogalym). The observed pattern in Na, Cl, and SO_4 concentrations also refutes the possibility of element leaching from frozen saline sediments abundant in the Russian Arctic Coast (e.g., Brouchkov, 2002), especially within the Tazovksy region (Nazarov, 2007). Overall, the influence of salts in surrounding rocks becomes to be pronounced in the ecosystems located north of 68°N (Dubikov, 2002), rocks which are outside of the study region.

To explain the observed element concentration pattern across the latitude we suggest, in accordance with results on DOC and CO_2 discussed in previous section, that higher reactivity of peat in suprapermafrost waters of the northern continuous permafrost sites may be responsible for elevated concentrations of most elements compared to southern sites of discontinuous sporadic and isolated permafrost. The release of major and trace elements from the bulk of the peat is essentially controlled by concentration of dissolved organic carbon and Al or Fe. Indeed, organo-Al-Fe colloids are recognized as the main carriers of many trace elements in low-TDS humic surface waters of permafrost-affected WSL territory (Pokrovsky et al., 2016b; Loiko et al., 2017). This is similar to boreal regions (Köhler et al., 2014). In studied supra-

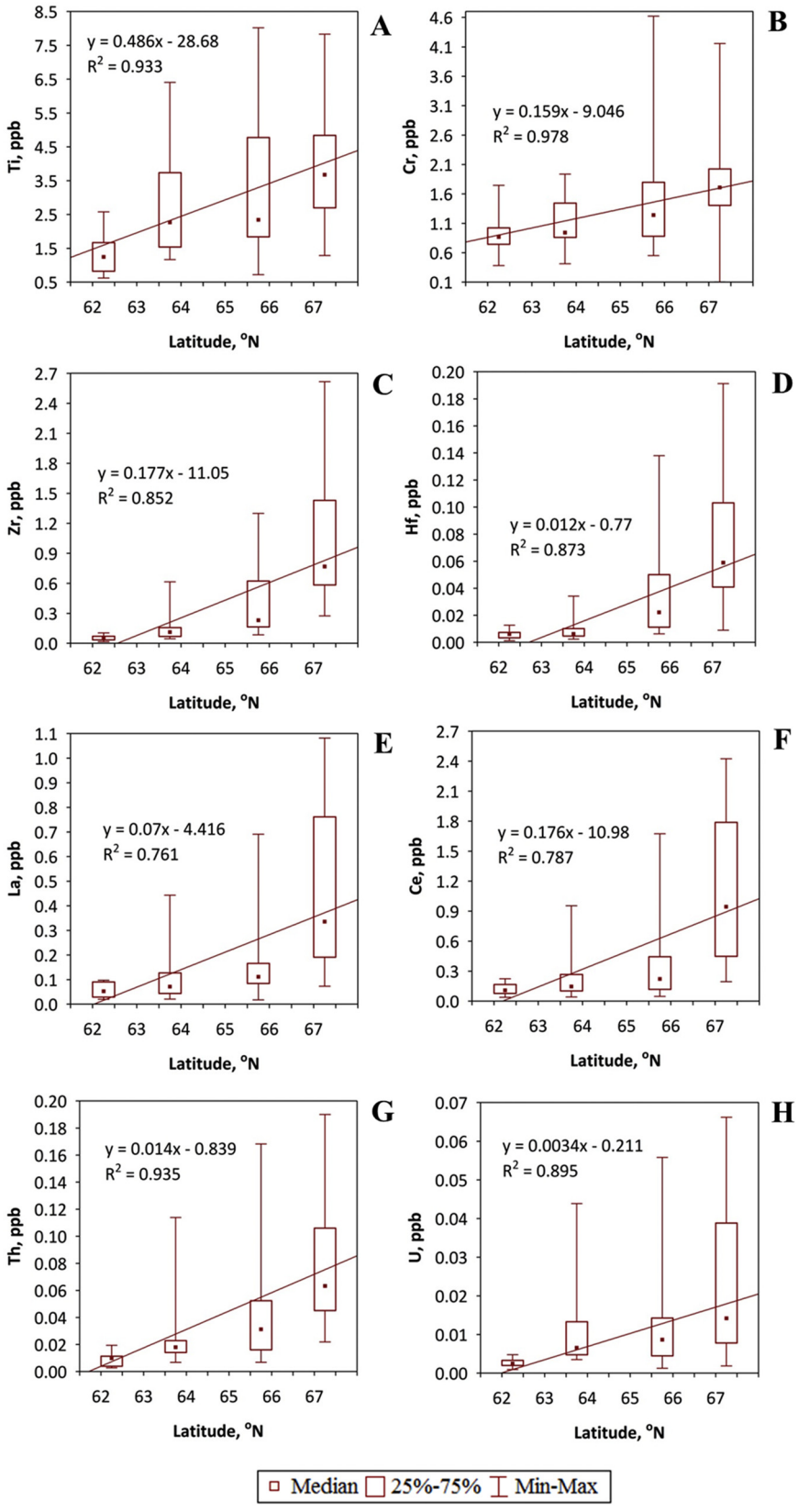

Fig. 6. Trace element (Ti, Cr, Zr, Hf, La, Ce, Th, U) concentration (μg/L) in suprapermafrost waters of the WSL as a function of latitude. The solid lines are linear regressions run over all micro-landscapes.

permafrost waters, Al concentration significantly correlates with many insoluble lithogenic trace elements such as Ti, V, Cr, Ga, Zr, Nb, REEs, Hf, and Th. Given that the mineral layer underlying the peat core is frozen weathering of underlaying mineral substrate is unlikely. Although peat mounds have higher distance between the ALT boundary and the mineral horizon, the concentration of lithogenic elements (Si,

Table 3
Latitudinal trends of average elemental concentrations in supra-permafrost waters of two main habitats across the permafrost gradient. The DOC, DIC, Cl, SO_4, Si, Ca, Mg, Na, K, P, Al, and Fe concentrations are in mg/L with all other trace elements reported in μg/L.

Element	Microlandscape	Equation	R^2	p-Value
CO_2	Hollow	$[CO_2] = 32.87x - 1716.6$	0.23	0.14
(μmol/L)	Subsidence/frost crack	$[CO_2] = 97.225x - 5672.1$	0.96	0.048
CH_4	Hollow	$[CH_4] = -1{,}206x + 86{,}03$	0.34	0.55
(μmol/L)	Subsidence/frost crack	$[CH_4] = 1.187x - 69.165$	0.08	0.61
pH	Hollow	$[pH] = 0.117L - 3.84$	0.50	0.0007
	Mound/polygon	$[pH] = 0.073L - 0.904$	0.62	0.0001
Cond	Hollow	$[Cond] = -1.882L + 176.71$	0.25	0.59
μS/cm	Mound/polygon	$[Cond] = -5.207L + 410.4$	0.58	0.0004
DOC	Hollow	$[DOC] = 4.336L - 229.23$	0.82	0.002
	Mound/polygon	$[DOC] = 4.317L - 195.6$	0.35	0.18
DIC	Hollow	$[DIC] = 0.031L - 0.244$	0.06	0.61
	Mound/polygon	$[DIC] = 0.116L - 5.865$	0.81	0.042
SO_4^{2-}	Hollow	$[SO_4^{2-}] = 0.195L - 11.93$	0.89	0.002
	Mound/polygon	$[SO_4^{2-}] = 0.1503L - 9.108$	0.66	0.42
Li	Hollow	$[Li] = = 0.1605L - 9.652$	0.81	0.002
	Mound/polygon	$[Li] = 0.099L - 5.742$	0.54	0.012
Na	Hollow	$[Na] = -0.029L + 2.252$	0.83	0.032
	Mound/polygon	$[Na] = -0.016L + 1.351$	0.31	0.35
Mg	Hollow	$[Mg] = 0.098L - 6.008$	0.83	<0.001
	Mound/polygon	$[Mg] = 0.108L - 6.629$	0.85	<0.001
Al	Hollow	$[Al] = 0.055L - 3.294$	0.57	0.035
	Mound/polygon	$[Al] = 0.127L - 7.736$	0.89	<0.001
Si	Hollow	$[Si] = 0.379L - 22.762$	0.84	<0.001
	Mound/polygon	$[Si] = 0.494L - 29.325$	0.87	0.002
P	Hollow	$[P] = -0.011L + 0.923$	0.50	0.62
	Mound/polygon	$[P] = -0.042L + 2.988$	0.81	0.009
K	Hollow	$[K] = -0.056L + 4.058$	0.56	0.59
	Mound/polygon	$[K] = -0.056L + 4.008$	0.69	0.057
Ca	Hollow	$[Ca] = 0.437L - 26.96$	0.57	<0.001
	Mound/polygon	$[Ca] = 0.799L - 50.025$	0.67	<0.001
Fe	Hollow	$[Fe] = 0.252L - 15.307$	0.94	<0.001
	Mound/polygon	$[Fe] = 0.276L - 16.65$	0.54	0.04
Ti	Hollow	$[Ti] = 0.374L - 21.786$	0.54	<0.001
	Mound/polygon	$[Ti] = 0.491L - 28.521$	0.77	0.006
V	Hollow	$[V] = 0.396L - 24.713$	0.56	<0.001
	Mound/polygon	$[V] = 0.778L - 48.701$	0.61	<0.001
Mn	Hollow	$[Mn] = 22.464L - 1415.7$	0.62	0.002
	Mound/polygon	$[Mn] = 35.65L - 2251.8$	0.64	0.002
Cr	Hollow	$[Cr] = 0.085L - 4.426$	0.82	<0.001
	Mound/polygon	$[Cr] = 0.141L - 7.728$	0.81	0.032
Co	Hollow	$[Co] = 0.321L - 20.045$	0.94	<0.001
	Mound/polygon	$[Co] = 0.437L - 27.286$	0.90	<0.001
Ni	Hollow	$[Ni] = 0.543L - 33.228$	0.98	<0.001
	Mound/polygon	$[Ni] = 0.995L - 61.938$	0.92	<0.001
Cu	Hollow	$[Cu] = 0.194L - 11.22$	0.28	0.46
	Mound/polygon	$[Cu] = 0.479L - 29.74$	0.58	<0.001
Zn	Hollow	$[Zn] = -0.589L + 48.346$	0.60	0.21
	Mound/polygon	$[Zn] = -0.583L + 45.335$	0.48	0.15
Ga	Hollow	$[Ga] = 0.006L - 0.357$	0.44	<0.001
	Mound/polygon	$[Ga] = 0.005L - 0.262$	0.47	0.217
As	Hollow	$[As] = 0.177L - 10.507$	0.56	<0.001
	Mound/polygon	$[As] = 0.641L - 39.769$	0.78	<0.001
Rb	Hollow	$[Rb] = 0.0478L - 2.453$	0.91	0.005
	Mound/polygon	$[Rb] = 0.025L - 0.759$	0.04	0.57
Sr	Hollow	$[Sr] = 2.428L - 148.02$	0.88	<0.001
	Mound/polygon	$[Sr] = 4.035L - 248.52$	0.82	<0.001
Zr	Hollow	$[Zr] = 0.118L - 7.366$	0.90	<0.001
	Mound/polygon	$[Zr] = 0.228L - 14.328$	0.81	<0.001
Mo	Hollow	$[Mo] = 0.005L - 0.288$	0.43	<0.001
	Mound/polygon	$[Mo] = 0.0147L - 0.903$	0.95	<0.001
Cd	Hollow	$[Cd] = -0.001L + 0.108$	0.01	0.45
	Mound/polygon	$[Cd] = 0.0048L - 0.258$	0.44	0.66
Sb	Hollow	$[Sb] = -0.006L + 0.453$	0.74	0.02
	Mound/polygon	$[Sb] = -0.0026L + 0.21$	0.26	0.2
Cs	Hollow	$[Cs] = -0.0018L + 0.138$	0.40	0.27
	Mound/polygon	$[Cs] = -0.0027L + 0.205$	0.27	0.06
Ba	Hollow	$[Ba] = 0.676L - 27.07$	0.81	0.03
	Mound/polygon	$[Ba] = 1.617L - 86.88$	0.46	0.03
La	Hollow	$[La] = 0.044L - 2.686$	0.56	<0.001
	Mound/polygon	$[La] = 0.116L - 7.272$	0.64	<0.001
Nb	Hollow	$[Nb] = 0.006L - 0.37$	0.83	<0.001
	Mound/polygon	$[Nb] = 0.011L - 0.666$	0.90	<0.001
Ce	Hollow	$[Ce] = 0.122L - 7.468$	0.66	<0.001
	Mound/polygon	$[Ce] = 0.291L - 18.172$	0.80	<0.001

Table 3 (*continued*)

Element	Microlandscape	Equation	R^2	p-Value
Pr	Hollow	[Pr] = 0.0169L − 1.045	0.65	<0.001
	Mound/polygon	[Pr] = 0.0373L − 2.339	0.70	<0.001
Nd	Hollow	[Nd] = 0.076L − 4.732	0.70	<0.001
	Mound/polygon	[Nd] = 0.155L − 9.731	0.62	<0.001
Sm	Hollow	[Sm] = 0.017L − 1.078	0.65	<0.001
	Mound/polygon	[Sm] = 0.036L − 2.225	0.62	<0.001
Eu	Hollow	[Eu] = 0.004L − 0.259	0.69	<0.001
	Mound/polygon	[Eu] = 0.009L − 0.559	0.70	<0.001
Gd	Hollow	[Gd] = 0.019L − 1.169	0.65	<0.001
	Mound/polygon	[Gd] = 0.038L − 2.392	0.62	<0.001
Tb	Hollow	[Tb] = 0.003L − 0.169	0.70	<0.001
	Mound/polygon	[Tb] = 0.006L − 0.347	0.64	<0.001
Dy	Hollow	[Dy] = 0.0157L − 0.979	0.65	<0.001
	Mound/polygon	[Dy] = 0.0325L − 2.044	0.61	<0.001
Ho	Hollow	[Ho] = 0.0033L − 0.203	0.65	<0.001
	Mound/polygon	[Ho] = 0.0064L − 0.404	0.61	<0.001
Er	Hollow	[Er] = 0.0102L − 0.638	0.66	<0.001
	Mound/polygon	[Er = 0.0204L − 1.282	0.68	<0.001
Yb	Hollow	[Yb] = 0.011L − 0.703	0.82	<0.001
	Mound/polygon	[Yb] = 0.02L − 1.264	0.66	<0.001
Lu	Hollow	[Lu] = 0.0016L − 0.101	0.63	<0.001
	Mound/polygon	[Lu] = 0.003L − 0.193	0.65	<0.001
Hf	Hollow	[Hf] = 0.008L − 0.496	0.90	<0.001
	Mound/polygon	[Hf] = 0.015L − 0.963	0.79	<0.001
W	Hollow	[W] = −0.0018L + 0.13	0.85	0.03
	Mound/polygon	[W] = −0.0014L + 0.103	0.87	0.09
Tl	Hollow	[Tl] = 0.0005L − 0.026	0.46	0.008
	Mound/polygon	[Tl] = 0.0016L − 0.097	1.00	0.003
Th	Hollow	[Th] = 0.008L − 0.483	0.59	<0.001
	Mound/polygon	[Th] = 0.019L − 1.205	0.88	<0.001
U	Hollow	[U] = 0.003L − 0.18	0.76	0.04
	Mound/polygon	[U] = 0.0056L − 0.348	0.86	<0.001
Pb	Hollow	[Pb] = −0.0782L + 5.838	0.47	0.26
	Mound/polygon	[Pb] = −0.0326L + 2.549	0.47	0.18

Al, V, Sr, REE, Zr, Hf, Th) in supra-permafrost water of the peat mounds is 1.3 to 3 times higher than that in hollows and subsidences (Table 2). Therefore, leaching of elements from mineral horizons does not impact active layer waters and the most likely source of lithogenic elements in peat cores is atmospheric deposition of silicate dust. This hypothesis is in agreement with former studies in western Siberia (Stepanova et al., 2015; Shevchenko et al., 2017) and other peat bogs (Shotyk, 1996; Shotyk et al., 2001). Because the studied supra-permafrost waters are acidic (pH ≤ 4) the solid aerosol particles may exhibit high reactivity in the peat profile either via bulk dissolution or surface desorption of metals (Shotyk et al., 2016).

In contrast, the biologically-indifferent elements delivered to the peat surface in soluble form from the atmosphere (Na, Cl, SO_4, Cs, W) and the micronutrients/toxicants (K, Rb, Cu, Zn, Sb, Cd, Pb) exhibited rather constant concentrations or a northward decreasing trend. We explain the lack of climate and permafrost impact on these elemental concentrations in supra-permafrost waters by similar atmospheric deposition and uptake by moss and lichen biomass (notably K, Rb, Zn) across the studied permafrost gradient. Indeed, the atmospheric influx of Cu, Zn, Sb, Cd, Pb, Cs, W to the peatbog surface is very high and strongly exceeds their export by rivers of the WSL (i.e., Shevchenko et al., 2017). Shevchenko et al. (2017) also showed that concentrations of these elements in atmospheric aerosols are similar across a sizeable latitudinal gradient of the WSL.

Overall, the major and trace element concentrations of WSL supra-permafrost waters reflect 2 main processes: (1) lithogenic element leaching from silicate dust and insoluble atmospheric aerosols deposited within the peat layer and at the moss/lichen surface, and (2) release of trace micronutrients and atmospheric toxicants from the peat and surface vegetation and their downward migration until the permafrost boundary (Fig. 8). The 1st process is strongly controlled by the presence of organic and organo aluminum colloids and thus enhances northward, with increase of DOC and Al level in the supra-permafrost waters, whereas the 2nd process is independent of DOC level and tightly linked to peat and moss chemical composition and reactivity. Element mobilization is also controlled by intensity of atmospheric input of soluble elements onto the moss and lichen surface. Unfortunately, lack of data on trace element concentrations in peat of the northern part of WSL prohibits testing the impact of peat chemical composition on soil waters across the latitudinal gradient studied. As summarized in Fig. 8, an overall export flux of elements from the peat column to the river in the northern site is higher than that in the south due to a combination of higher stocks of elements and a higher degree of element mobilization from the peat to the soil water. In particular, higher concentrations of organic and organo-mineral colloids, denser peat, and higher residence times of water in the northern sites can be responsible for the difference in possible export fluxes.

4.3. The role of local micro-landscape in element concentration in supra-permafrost waters

From previous hydrological studies of WSL peat bogs (Novikov et al., 2009), it is known that the positive (mounds, polygons) and negative (hollows, depressions, subsidences and frost cracks) forms of microrelief have dramatically different water transfer regimes. In spring, the hollows receive the melted snow which was accumulated there over the winter whereas in summer they receive the rain water via supra-permafrost flow along the permafrost table. As a result, the hollows and depressions are essentially responsible for delivering the water, organic carbon, and solutes to the adjacent rivers and lakes. In contrast, the mounds and polygons receive water via snowmelt effectively in spring. In summer, this water is subjected to evaporation and uptake by plants leading to enrichment of pore fluids in some elements indifferent to plants.

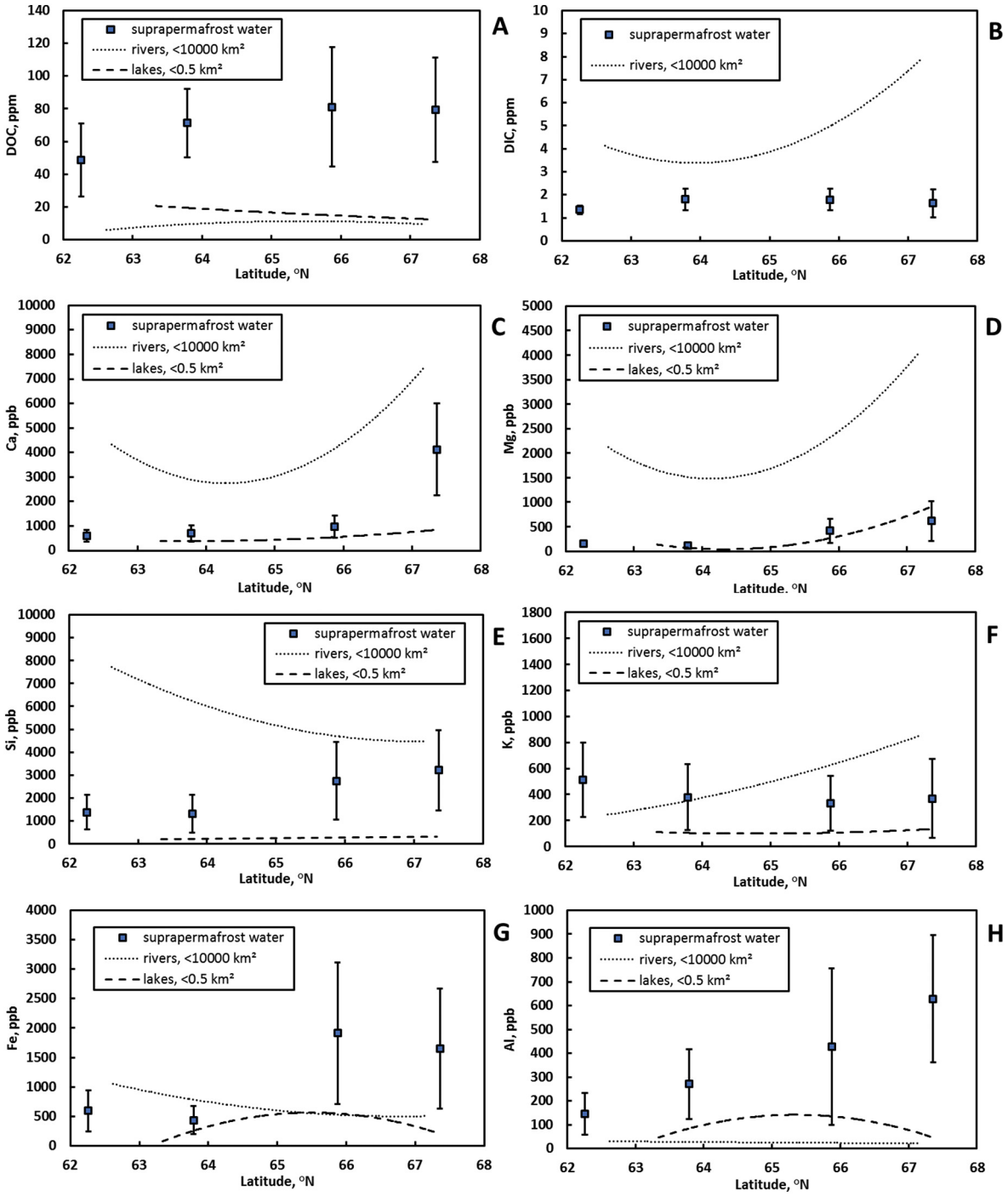

Fig. 7. DOC (A), Si (B), Ca (C), Mg (D), Fe (E)€, Al (F), Ni (G), and Mo (H) concentrations in rivers (dotted line), lakes (dashed line), and supra-permafrost waters (filled squares) across the latitudinal gradient of the WSL.

The possible role of underlying mineral horizons in DOC control in supra-permafrost waters can be evaluated via analyzing the position of ALT relative to the mineral horizon of the soil/peat column. Although the ALT is 2 (mounds/polygons) to 4 (depressions) times greater in Khanymey (discontinuous sporadic permafrost) compared to Tazovsky (continuous permafrost), all supra-permafrost waters sampled in this study were collected from peat and not mineral horizons. The distance between the depth of supra-permafrost water horizons located at the border between thawed and frozen peat and underlying mineral horizon in mounds/polygons ranged from 0 to 350 cm with an average value of 60 cm and was not linked to the latitude at date of sampling. This distance in hollows is sizably lower (0 to 240 cm with an average value of 24 cm). As such, it is possible the 1.5 ± 0.2 times higher DOC concentrations in mounds relative to hollows across the WSL transect (Fig. 2A) is due to retention of part of the soil water DOM on underlying mineral layers.

We hypothesize that the water residence time in various microlandscapes determines the pattern of element concentration in supra-permafrost water. In fact, the DOC concentration in peat palsa catchment outflows in discontinuous permafrost zone decreases with the increase in runoff (Olefeldt and Roulet, 2012). The supra-permafrost waters in hollows should have shorter residence time compared to mounds. Thus, lateral water flow rate in the first 0–10 cm layer of hollows and depressions is 7 to 30 times (and on average 20 times) higher

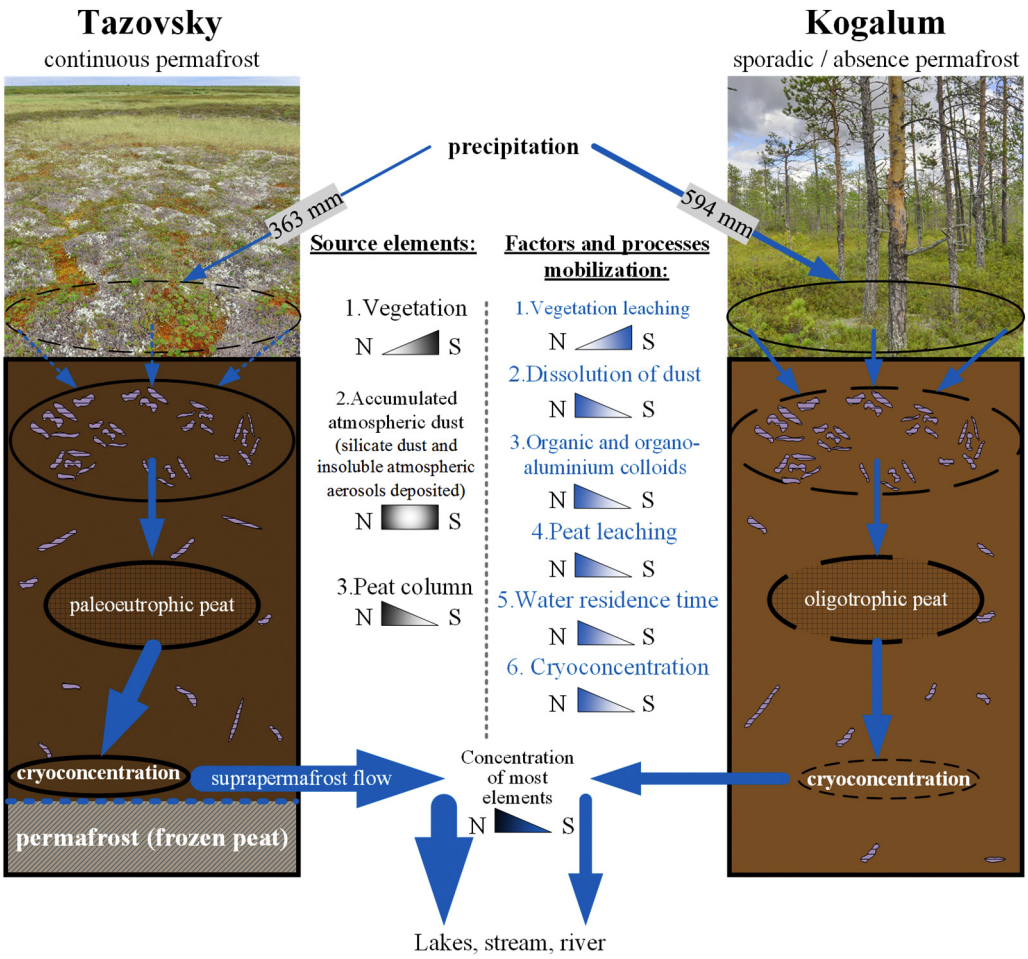

Fig. 8. An illustration of supra-permafrost water enrichment in DOC and elements in two contrasting test sites – Kogalym of sporadic/isolated permafrost (right) and Tazovsky of continuous permafrost (left). N and S represent North and South, respectively. The thickness of arrows reflects degree of enrichment in solutes after the water travels through the peat column. The acute end of the triangle shows for which site the corresponding factor of enrichment plays a more important role.

than that in mounds as determined by NaCl tracing in our field experiments, which is consistent with available literature data (Batuev, 2012). As a result, higher local runoff and hydraulic conductivity of hollows and depressions compared to mounds are responsible for lower DOC and metal concentrations in waters from mounds and polygons compared to hollows, depressions, subsidences, and frost cracks.

Another reason for enrichment in DOC and dissolved metals of the waters in mounds compared to hollows or subsidences may be due to cryoconcentration of solutes during soil water freezing (Kokelj et al., 2002; Ireson et al., 2013; Jessen et al., 2014). Cryoconcentration is expected to be much stronger in mounds compared to hollows given the much lower temperatures (Koronatova et al., 2015; Matyshak et al., 2017). In addition, cryoconcentration of soluble salts (Mg, Na, SO_4, Cl) should be more efficient in the north relative to the south as was previously demonstrated for deep groundwaters in the region (Ivanov and Beshentsev, 2005).

4.4. Supra-permafrost waters as source of DOC, major and trace elements to small rivers and thermokarst lakes of WSL

The hydrological continuum of peat active layer waters and those of adjacent rivers and lakes implies that the main feeding of open surface water bodies is from surrounding soils delivering their solutes via supra-permafrost flow (Fig. 1). There is a notable similarity in the latitudinal trends of some major and trace elements between lakes, rivers, and supra-permafrost waters illustrated in Figs. 7 and S4 for Ca, Mg, Ni, Mo, and Sb. Moreover, the concentrations of DOC and most elements in thermokarst lakes during the summer are always lower or comparable to those of supra-permafrost waters across the latitudinal gradient of permafrost-affected regions. This first-order comparison demonstrates that the supra-permafrost waters are capable of providing the concentrations of all major and trace elements in surface waters. In other words, the transport of active layer water along the permafrost boundary in the form of supra-permafrost flow may be the sole source of incoming solutes to thermokarst lakes of western Siberia during summer periods. This hypothesis is consistent with the lack of underground feeding for WSL thermokarst lakes demonstrated in earlier studies (Manasypov et al., 2015).

In contrast to lakes, WSL rivers exhibit concentrations of DIC, Ca, Mg, Na, Si, Al, Sr, and Mn that were higher than those in the supra-permafrost flow (Figs. 7 and S4 of Supplement). This requires some underground "mineral" influx into the rivers in addition to surface and shallow subsurface "organic" flux. Similar to other permafrost-bearing peatlands (Malov et al., 2015), this underground water influx reflects water-sedimentary rock (sandstone, siltsone, and/or limestone) interaction at certain depth and may occur via taliks under the river bed and shallow subsurface flow over clay and silt deposits.

An important consequence of the results obtained on supra-permafrost waters in the WSL is that the intensity of chemical weathering and associated CO_2 consumption in the permafrost zone (i.e., Smedberg et al., 2006; Beaulieu et al., 2012) may be dramatically different between various regions and between large and small rivers. The chemical weathering in small catchments ($S_{watershed} < 1000$ km^2) without pronounced underground feeding in frozen peatlands could

be overestimated relative to regions with shallow organic soil horizons. The summer time concentration of DIC, Ca, Mg, K, and Si in small rivers located between 62 and 66°N in discontinuous permafrost zones are comparable (±50%) to the concentration of these elements in supra-permafrost waters in adjacent peat plateaus where the mineral horizon is frozen and does not participate in chemical weathering. As a result, the flux of DIC and major cations in the peatland-draining rivers should be corrected for the input of these elements from non-mineral sources. For a number of small rivers in the permafrost zone of the WSL that are fed by supra-permafrost flux through the peat horizon, this correction can range from 20 to 90% for DIC, Ca, and Mg. The overall Northern Eurasia territory affected by these corrections may be as large as 2 million km^2 and includes the western Siberia, NE European palsa peatlands, Northern Siberian, Anabar, Yana-Indigirka, and Kolyma lowlands.

4.5. Prospective for climate change in western Siberia

There are two main scenarios of climate warming impact on western Siberian peatlands. According to the first scenario, the area of hollows and subsidences will increase and the coverage of palsa by mounds and polygons will be decreasing (Moskalenko, 2012; Pastukhov and Kaverin, 2016; Pastukhov et al., 2016). Because the supra-permafrost waters in mounds are generally 50% richer in DOC and metals compared to hollows this will produce sizeable decrease of the overall stock of dissolved carbon and metals in inland waters of the WSL. The second scenario assumes no change in micro-relief distribution but northward retreat of the permafrost boundary and the increase of the ALT (Sherstyukov and Sherstyukov, 2015; Reshetko and Moiseeva, 2016). This latitudinal shift will also decrease the DOC and elemental concentrations in supra-permafrost waters of the northern region. Combining both scenarios, one can expect 1) fast migration of the permafrost boundary via increase of the ALT without micro-landscape change and 2) after several hundred years (necessary to form a new peat layer at least 20 cm thick) a replacement of mounds by hollows. The decade to century period are reported to be needed for reorganization of vegetation, water storage, and flow paths in the permafrost landscapes in peaty-silt lowlands (Jorgenson et al., 2013). The combined effect on DOC and metal concentration decreases in supra-permafrost waters of continuous permafrost regions may range between a factor of 2 and 5.

The CO_2 behavior is however different from that of DOC and soluble elements since its concentration was 2.5 ± 1.0 times higher in permafrost subsidences and frost cracks compared to hollows. Under the scenario of climate change, the relative proportion of hollows will increase and the permafrost subsidences and frost cracks may disappear because the hydraulic conductivity between negative forms of micro-relief may increase (Tyrtikov, 1973; Lupachev et al., 2016). This will lead to an overall decrease in CO_2 concentration in supra-permafrost waters of the WSL, although this decrease will be smaller than that of DOC and metals.

Other modifications linked to the climate change in WSL permafrost-affected zones such as the change of global hydrological regime of large (>10,000 km^2 watershed area) rivers (White et al., 2007; Karlsson et al., 2014, 2015) consisting of the increase in winter baseflow (Yang et al., 2004) and increase of groundwater feeding (Frey et al., 2007a, 2007b) are unlikely to appreciably modify the supra-permafrost water chemistry. A secondary effect of these changes may be an increasing the difference between mound and hollow/depression due to the change of the hydrological pathway, and, consequently, water residence time in peat pore space. However, it is impossible to predict to which degree changes in the hydrological regimes of winter baseflow and spring flooding can affect water dynamics in peat soils during August, the period of maximal ALT. Based on obtained data from contrasting microenvironments of the same site (Fig. 2, Table 2), forecasted changes will be within a factor of 2 which is comparable with the dispersity of in-situ element concentrations in different micro-landscapes.

Finally, the increase in vegetation productivity reported for Arctic river watersheds (Sturm et al., 2001; Tape et al., 2006; Kirdyanov et al., 2012; Abbott et al., 2016) will most likely proportionally increase the downward flux of macronutrients originated from decomposition (leaching) of plant litter at the beginning of the summer season whereas at the end of season the maximal rooting depth may favor preferential uptake of K, Rb, Si, Mn, Ba, and other micronutrients. However, due to compensation of processes oriented in different directions, the overall modification of the element storage in supra-permafrost waters of discontinuous/continuous permafrost zone may be smaller than those projected by simple latitudinal shift.

The climate change in western Siberia is likely to cause a shift of the permafrost boundary northward and increase in active layer thickness (Pavlov and Moskalenko, 2002; Frey and Smith, 2003; Romanovsky et al., 2010; Vasiliev et al., 2011; Anisimov et al., 2013). Using a substituting space for time scenario and considering the most extreme shift of the permafrost boundary by 4° to the north, we foresee a two-fold decrease in CO_2, Al, Mg, Ca, Si, Fe, a number of trace micronutrients (Ni, Co, Cu, V, Cr, Sr, Mo), and low mobile trivalent and tetravalent elemental concentrations in the supra-permafrost waters of the continuous permafrost zone. Concentrations of CH_4, DIC, Na, K, Cl, SO_4, Rb, Cs, Sb, W, Zn, Ba, Cd, and Pb will likely remain constant. These predictions however, have to be taken with caution, especially within the short-term scenario as 1) the main warming in WSL is due to winter temperature rise (Matyshak et al., 2017), which should weakly affect the soil regime, and 2) the warming in this region has currently slowed down and is unlikely to be strongly pronounced in the near future with the exception being a slow rise in river discharge (Paromov et al., 2017).

5. Concluding remarks

We observed a sizeable latitudinal trend of CO_2, DOC, and a number of major and trace elements in in supra-permafrost waters sampled in 4 representative permafrost zones of the northern WSL. Contrary to an expected decrease of concentrations northward — with decrease of MAT, ALT, vegetation and an increase in permafrost thickness and coverage — most solutes of supra-permafrost waters exhibited higher concentrations in northern sites compared to southern sites. Specifically, there was a net northward increasing trend in concentrations of DOC, CO_2, Si, Al, Mg, Ca, Fe, Mn, Ni, Cu, Sr, Co, Ti, Cr, V, Ga, As, Zr, Nb, Mo, REEs, Hf, Tl, Th, and U with distinctly higher concentrations of these components in continuous permafrost zones relative to discontinuous and sporadic permafrost zones. A constant or northward decreasing concentration of CH_4, specific conductivity, DIC, $SUVA_{280}$, Cl, SO_4, P, K, Cu, Zn, Cd, Pb, Sb, Cs, Ba and W was observed across a latitudinal gradient. This latitudinal trend of elemental concentrations in supra-permafrost peat waters was generally in agreement with that observed earlier in river and lake waters across the same latitudinal gradient.

The higher DOC north of 66°N in the continuous permafrost zone (nearly 1.5 times higher than DOC in discontinuous to sporadic zones) was consistent with elevated CO_2 concentrations in northern sites, although DOC and CO_2 concentrations were not correlative. Because the main source of water and solutes in the river is influx via supra-permafrost flow over the frozen layer, the concentration trend of active layer waters sampled in this work were compared with average riverine concentrations. A number of elements exhibited reasonable consistency in their concentration values and northward (>65°N) increasing concentration trends in rivers and supra-permafrost waters: Ca, Mg, Sr, Ni, Cu, Mo, REE, and U.

The role of micro-relief (mound or polygon versus hollow or crack) was subordinate relative to the latitudinal position of the sampling site. However, the DOC, Si, Al, Fe, V, As, and Sr concentrations were systematically higher in mounds relative to hollows (by a factor of 1.4 to

3.0) whereas the other elements did not exhibit significant difference between micro-landscapes.

We conclude that the overall export fluxes of DOC, major cations, Si, and trace metals from the peatland to the hydrological network is defined by the amount of water that passes through the unfrozen peat column until the permafrost boundary before being evacuated to the river. This prediction is consistent with reported higher riverine fluxes of DOC, Si, and cations in the northern region of WSL (67 ± 0.5°N) relative to the southern region (62–65°N) of western Siberia peat (Pokrovsky et al., 2015). It is therefore possible that the shift of the permafrost boundary northward due to climate warming may decrease the GHG, DOC, and metal concentrations in peat soil waters and export fluxes from the land to the ocean.

Acknowledgements

We acknowledge support from RFFI grants No 16-34-60203-mol_a_dk, 16-54-16005, 17-55-16008, and RNF grant No 18-17-00237 “Mechanisms of hydrochemical runoff”. Chris Benker is thanked for editing the English of the manuscript.

Appendix A. Supplementary data

Supplementary data to this article can be found online at https://doi.org/10.1016/j.scitotenv.2018.04.059.

References

Abbott, B.W., Jones, J.B., Schuur, E.A.G., Chapin III, F.S., et al., 2016. Biomass offsets little or none of permafrost carbon release from soils, streams, and wildfire: an expert assessment. Environ. Res. Lett. 11 (3):034014. https://doi.org/10.1088/1748-9326/11/3/034014.

Akerman, H.J., Johansson, M., 2008. Thawing permafrost and thicker active layers in subarctic Sweden. Permafr. Periglac. Process. 19:279–292. https://doi.org/10.1002/ppp.626.

Anisimov, O., Kokorev, V., Zhil'tsova, Y., 2013. Temporal and spatial patterns of modern climatic warming: case study of northern Eurasia. Clim. Chang. 118:871–883. https://doi.org/10.1007/s10584-013-0697-4.

Anisimov, O.A., Zhiltcova, Y.L., Razzhivin, V.Y., 2015. Predictive modeling of plant productivity in the Russian Arctic using satellite data. Izv. Atmos. Oceanic Phys. 51 (9): 1051–1059. https://doi.org/10.1134/S0001433815090042.

Avagyan, A., Runkle, B.R.K., Hartmann, J., Kutzbach, L., 2014. Spatial variations in porewater biogeochemistry greatly exceed temporal changes during baseflow conditions in a boreal river valley mire complex, Northwest Russia. Wetlands 34:1171–1182. https://doi.org/10.1007/s13157-014-0576-4.

Batuev, V.I., 2012. Formation of water runoff from mound bogs (case study of western Siberia). TSPU Bull. 122 (7), 146–152.

Baulin, V.V., Belopukhova, E.B., Dubikov, G.I., Shmelev, L.M., 1967. Geocryological Conditions of Western Siberia Lowland. Nauka Publishing House, Moscow (in Russian).

Beaulieu, E., Godderis, Y., Donnadieu, Y., Labat, D., Roelandt, C., 2012. High sensitivity of the continental-weathering carbon dioxide sink to future climate change. Nat. Clim. Chang. 2:346–349. https://doi.org/10.1038/nclimate1419.

Beilman, D.W., MacDonald, G.M., Smith, L.C., Reimer, P.J., 2009. Carbon accumulation in peatlands of West Siberia over the last 2000 years. Glob. Biogeochem. Cycles 23 (GB1012). https://doi.org/10.1029/2007GB003112.

Bendell-Young, L., 2003. Peatland interstitial water chemistry in relation to that of surface pools along a peatland mineral gradient. Water Air Soil Pollut. 143 (1–4):363–375. https://doi.org/10.1023/A:1022865109409.

Botch, M.S., Kobak, K.I., Vinson, T.S., Kolchugina, T.P., 1995. Carbon pools and accumulation in peatlands of the former Soviet Union. Glob. Biogeochem. Cycles 9:37–46. https://doi.org/10.1029/94GB03156.

Brouchkov, A., 2002. Nature and distribution of frozen saline sediments on the Russian Arctic coast. Permafr. Periglac. Process. 13:83–90. https://doi.org/10.1002/ppp.411.

Brown, J., Ferrians Jr, O.J., Heginbottom, J.A., Melnikov, E.S., 2001. Circum-arctic map of permafrost and ground ice conditions, Boulder, CO 80309-0449 USA. National Snow and Ice Data Center, Digital media, 1998.

Čapek, P., Diakova, K., Dickopp, J.E., Barta, J., Wild, B., Schnecker, J., et al., 2015. The effect of warming on the vulnerability of subducted organic carbon in arctic soils. Soil Biol. Biochem. 90:19–29. https://doi.org/10.1016/j.soilbio.2015.07.013.

Carey, S.K., 2003. Dissolved organic carbon fluxes in a discontinuous permafrost subarctic alpine catchment. Permafr. Periglac. Process. 14 (2), 161–171.

De la Cruz, O., Holmes, S., 2011. The duality diagram in data analysis: examples of modern applications. Ann. Appl. Stat. 5 (4):2266–2277. https://doi.org/10.1214/10-AOAS408.

Dean, J.F., Billett, M.F., Baxter, R., Dinsmore, K.J., Lessels, J.S., Street, L.E., Subke, J.-A., Tetzlaff, D., Washbourne, I., Wookey, P.A., 2016. Biogeochemistry of “pristine” freshwater stream and lake systems in the western Canadian Arctic. Biogeochemistry 130 (3):191–213. https://doi.org/10.1007/s10533-016-0252-2.

Dielemann, C.M., Lindo, Z., McLaughlin, J.W., Craig, A.E., Branfireum, B.A., 2016. Climate change effects on peatland decomposition and porewater dissolved organic carbon biogeochemistry. Biogeochemistry 128:385–396. https://doi.org/10.1007/s10533-016-0214-8.

Drozdov, D.S., Ukraintseva, N.G., Tsarev, A.M., Chekrygina, S.N., 2010. Change of permafrost temperature field and geosystem state on the Urengoy oil-gas-field territory during the last 35 years (1974–2008). Earth Cryosphere 14 (1), 22–31.

Dubikov, G.I., 2002. Composition and Cryogenic Structure of Permafrost in West Siberia. GEOS Publishing House, Moscow (in Russian).

Fotiev, S.M., 1989. Taliks and their formations. In: Ershov, E.D. (Ed.), Geocryology of the USSR, Western Siberia, Publishing House Nedra, Moscow, pp. 72–84 (in Russian).

Fotiev, S.M., 1991. Formation of taliks of Western Siberia. Permanently Frozen Rocks and Cryogenic Processes. Publishing House Nauka, Moscow, pp. 71–78 (in Russian).

Frampton, A., Destouni, G., 2015. Impact of degrading permafrost on subsurface solute transport pathways and travel times. Water Resour. Res. 51:7680–7701. https://doi.org/10.1002/2014WR016689.

Frey, K.E., Smith, L.C., 2003. Recent temperature and precipitation increases in West Siberia and their association with the Arctic Oscillation. Polar Res. 22 (2), 287–300.

Frey, K.E., Smith, L.C., 2005. Amplified carbon release from vast west Siberian peatlands by 2100. Geophys. Res. Lett. 32, L09401. https://doi.org/10.1029/2004GL022025.

Frey, K.E., Smith, L.C., 2007. How well do we know northern land cover? Comparison of four global vegetation and wetland products with a new ground-truth database for West Siberia. Glob. Biogeochem. Cycles 21, GB1016. https://doi.org/10.1029/2006GB002706.

Frey, K.E., McClelland, J.W., Holmes, R.M., Smith, L.C., 2007a. Impacts of climate warming and permafrost thaw on the riverine transport of nitrogen and phosphorus to the Kara Sea. J. Geophys. Res. 112, G04S58. https://doi.org/10.1029/2006JG000369.

Frey, K.E., Siegel, D.I., Smith, L.C., 2007b. Geochemistry of west Siberian streams and their potential response to permafrost degradation. Water Resour. Res. 43, W03406. https://doi.org/10.1029/2006WR004902.

Gangloff, S., Stille, P., Schmitt, A.D., Chabaux, F., 2016. Factors controlling the chemical composition of colloidal and dissolved fractions in soil solutions and the mobility of trace elements in soils. Geochim. Cosmochim. Acta 189:37–57. https://doi.org/10.1016/j.gca.2016.06.009.

Gentsch, N., Mikutta, R., Alves, R.J.E., et al., 2015. Storage and transformation of organic matter fractions in cryoturbated permafrost soils across the Siberian Arctic. Biogeosci. Discuss. 12:2697–2743. https://doi.org/10.5194/bg-12-4525-2015.

Giesler, R., Högberg, M.N., Strobel, B.W., Richter, A., Nordgren, A., Högberg, P., 2006. Production of dissolved organic carbon and low-molecular weight organic acids in soil solution driven by recent tree photosynthate. Biogeochemistry 84:1–12. https://doi.org/10.1007/s10533-007-9069-3.

Giesler, R., Lyon, S.W., Mörth, C.-M., Karlsson, J., Karlsson, E.M., Jantze, E.J., Destouni, G., Humborg, C., 2014. Catchment-scale dissolved carbon concentrations and export estimates across six subarctic streams in northern Sweden. Biogeosciences 11:525–537. https://doi.org/10.5194/bg-11-525-2014.

Griffiths, N., Sebestyen, S.D., 2016. Dynamic vertical profiles of peat porewater chemistry in a northern peatland. Wetlands 36 (6):1119–1130. https://doi.org/10.1007/s13157-016-0829-5.

Grosse, G., Goetz, S., McGuire, A.D., Romanovsky, V.E., Schuur, E.A.G., 2016. Changing permafrost in a warming world and feedbacks to the earth system. Environ. Res. Lett. 11, 040201. https://doi.org/10.1088/1748-9326/11/4/040201.

Guo, L., Ping, C.L., MacDonald, R.W., 2007. Mobilization pathways of organic carbon from permafrost to Arctic rivers in a changing climate. Geophys. Res. Lett. 34, L13603. https://doi.org/10.1029/2007GL030689.

Hodgkins, S.B., Tfaily, M.M., McCalley, C.K., Logan, T.A., Crill, P.M., Saleska, S.R., Rich, V.I., Chanton, J.P., 2014. Changes in peat chemistry associated with permafrost thaw increase greenhouse gas production. PNAS 111 (16):5819–5824. https://doi.org/10.1073/pnas.1314641111.

Ilina, I.S., Lapshina, E.I., Lavrenko, N.N., et al., 1985. Vegetation Cover of Western Siberian Plain. Publishing House Nauka, Novosibirsk (in Russian).

Ilina, S.M., Drozdova, O.Y., Lapitskiy, S.A., Alekhin, Y.V., Demin, V.V., Zavgorodnyaya, Yu.A., Shirokova, L.S., Viers, J., Pokrovsky, O.S., 2014. Size fractionation and optical properties of dissolved organic matter in the continuum soil solution-bog-river and terminal lake of a boreal watershed (North Karelia, Russia). Org. Geochem. 66, 14–24.

Ireson, A.M., van der Kamp, G., Ferguson, G., Nachshon, U., Wheater, H.S., 2013. Hydrogeological processes in seasonally frozen northern latitudes: understanding, gaps and challenges. Hydrogeol. J. 21:53–66. https://doi.org/10.1007/s10040-012-0916-5.

IUSS Working Group WRB, 2014. World reference base for soil resources 2014. International Soil Classification System for Naming Soils and Creating Legends for Soil Maps. World Soil Resources Reports No. 106. FAO, Rome.

Ivanov, Yu.K., Beshentsev, V.A., 2005. Paleo-geographical aspects of formation of chemical composition of fresh underground waters in Yamalo-Nenetz region. Lithosphere 4 (17), 188–196 (in Russian with English abstract).

Jantze, E.J., Lyon, S.W., Destouni, G., 2013. Subsurface release and transport of dissolved carbon in a discontinuous permafrost region. Hydrol. Earth Syst. Sci. 17:3827–3839. https://doi.org/10.5194/hess-17-3827-2013.

Jessen, S., Holmslykke, H.D., Rasmussen, K., Richardt, N., Holm, P.E., 2014. Hydrology and pore water chemistry in a permafrost wetland, Ilulissat, Greenland. Water Resour. Res. 50 (6):4760–4774. https://doi.org/10.1002/2013WR014376.

Johnson, K.D., Harden, J.W., McGuire, A.D., Clark, M., Yuan, F., Finley, A.O., 2013. Permafrost and organic layer interactions over a climate gradient in a discontinuous permafrost zone. Environ. Res. Lett. 8, 035028. https://doi.org/10.1088/1748-9326/8/3/035028.

Johnston, C.E., Ewing, S.A., Harden, J.W., Varner, R.K., Wickland, K.P., Koch, J.C., Fuller, C.C., Manies, K., Jorgenson, M.T., 2014. Effect of permafrost thaw on CO_2 and CH_4 exchange in a western Alaska peatland chronosequence. Environ. Res. Lett. 9 (8), 109601. https://doi.org/10.1088/1748-9326/9/8/085004.

Jorgenson, M.T., Harden, J., Kanevskiy, M., O'Donnell, J., Wickland, K., Ewing, S., Manies, K., Zhuang, Q., Shur, Y., Striegl, R., Koch, J., 2013. Reorganization of vegetation, hydrology and soil carbon after permafrost degradation across heterogeneous boreal landscapes. Environ. Res. Lett. 8, 035017. https://doi.org/10.1088/1748-9326/8/3/035017.

Karavanova, E.I., Malinina, M.S., 2007. Spatial and temporal variation in the elemental composition of soil solution from gleyic peaty-podzolic soils. Eurasian Soil Science. 40 (8):830–838. https://doi.org/10.1134/S1064229307080042.

Karlsson, J.M., Lyon, S.W., Destouni, G., 2014. Temporal behavior of lake size-distribution in a thawing permafrost landscape in Nothwestern Siberia. Remote Sens. 6:621–636. https://doi.org/10.3390/rs6010621.

Karlsson, J.M., Jaramillo, F., Destouni, G., 2015. Hydro-climatic and lake change patterns in Arctic permafrost and non-permafrost areas. J. Hydrol. 529:134–145. https://doi.org/10.1016/j.jhydrol.2015.07.005.

Kawahigashi, M., Kaiser, K., Kalbitz, K., Rodionov, A., Guggenberger, G., 2004. Dissolved organic matter in small streams along a gradient from discontinuous to continuous permafrost. Glob. Chang. Biol. 10:1576–1586. https://doi.org/10.1111/j.1365-2486.2004.00827.x.

Keller, K., Blum, J.D., Kling, G.W., 2010. Stream geochemistry as an indicator of increasing permafrost thaw depth in an Arctic watershed. Chem. Geol. 273:76–81. https://doi.org/10.1016/j.chemgeo.2010.02.013.

Kirdyanov, A.V., Hagedorn, F., Knorre, A.A., Fedotova, E.V., Vaganov, E.A., Naurzbaev, M.M., Moiseev, P.A., Rigling, A., 2012. 20th century tree-line advance and vegetation changes along an altitudinal transect in Putorana Mountains, northern Siberia. Boreas 41 (1):56–67. https://doi.org/10.1111/j.1502-3885.2011.00214.x.

Klinova, E.A., Faibusovich, Ya.E., Abakumova, L.A., 2012. State geological map of the Russian Federation at a scale of 1: 1,000,000. West Siberian Series. Map of the Pliocene-Quaternary formations, R-43 (Surgut). Cartographic factory VSEGEI, St. Petersburg (in Russian).

Koch, J.C., Runkel, R.L., Striegl, R., Mcknight, D.M., 2013. Hydrologic controls on the transport and cycling of carbon and nitrogen in a boreal catchment underlain by continuous permafrost. J. Geophys. Res. Biogeosci. 118, 698–712.

Köhler, S.J., Lidman, F., Laudon, H., 2014. Landscape types and pH control organic matter mediated mobilization of Al, Fe, U and La in boreal catchments. Geochim. Cosmochim. Acta 135:190–202. https://doi.org/10.1016/j.gca.2014.03.033.

Kokelj, S.V., Smith, C.A.S., Burn, C.R., 2002. Physical and chemical characteristics of the active layer and permafrost, Herschel Island, western Arctic Coast, Canada. Permafr. Periglac. Process. 13:171–185. https://doi.org/10.1002/ppp.417.

Koronatova, N.G., Stepanova, V.A., Kosykh, N.P., 2015. Temperature regime of the upper layer of frozen bogs of Western Siberia. In: Kabanov, M.V. (Ed.), Eleventh Siberian Meeting on Climate and Environmental Monitoring: Abstracts, Tomsk :pp. 43–44 (in Russian). http://www.imces.ru/media/uploads/CCKEM2015.pdf.

Kramarenko, V.V., Emel'yanova, T.Ya, 2009. Description of physical properties of high-moor peat in Tomsk region. Proc. Tomsk State Univ. 322:265–272 (in Russian). http://sun.tsu.ru/mminfo/000063105/322/image/322-265.pdf.

Kremenetski, K.V., Velichko, A.A., Borisova, O.K., MacDonald, G.M., Smith, L.C., Frey, K.E., Orlova, L.A., 2003. Peatlands of the West Siberian Lowlands: current knowledge on zonation, carbon content and late quaternary history. Quat. Sci. Rev. 22 (5–7): 703–723. https://doi.org/10.1016/S0277-3791(02)00196-8.

Lamhonwah, D., Lafrenière, M.J., Lamoureux, S.F., Wolfe, B.B., 2017. Evaluating the hydrological and hydrochemical responses of a high arctic catchment during an exceptionally warm summer. Hydrol. Process. 31, 2296–2313.

Liss, O.L., Abramova, L.I., Avetov, N.A., Berezina, N.A., Inisheva, L.I., Kurnishnikova, T.V., Sluka, Z.A., Tolpysheva, T.Yu., Shvedchikova, N.K., 2001. Wetland Systems of West Siberia and their Importance for Nature Conservation. Grif i K publisher, Tula, Russia (in Russian).

Liu, L., Chen, H., Zhu, Q., Yang, G., Zhu, E., Hu, J., Peng, C., Jiang, L., Zhan, W., Ma, T., He, Y., Zhu, D., 2016. Responses of peat carbon at different depths to simulated warming and oxidizing. Sci. Total Environ. 548–549:429–440. https://doi.org/10.1016/j.scitotenv.2015.11.149.

Loiko, S.V., Pokrovsky, O.S., Raudina, T.V., Lim, A., Kolesnichenko, L.G., Shirokova, L.S., Vorobyev, S.N., Kirpotin, S.N., 2017. Abrupt permafrost collapse enhances organic carbon, CO_2, nutrient and metal release into surface waters. Chem. Geol. 471, 153–165.

Lupachev, A.V., Gubin, S.V., Veremeeva, A.A., Kaverin, D.A., Pastukhov, A.V., Yakimov, A.S., 2016. Microrelief of the permafrost table: structure and ecological functions. Earth Cryosphere XX (2), 3–14 (in Russian).

Ma, R., Sun, X.Z., Hu, Y.L., Chang, Q.X., Wang, S., Xing, W.L., Ge, M.Y., 2017. Hydrological connectivity from glaciers to rivers in the Qinghai-Tibet Plateau: roles of suprapermafrost and subpermafrost groundwater. Hydrol. Earth Syst. Sci. 21 (9), 4803–4823.

Malov, A.I., Bolotov, I.N., Pokrovsky, O.S., Zykov, S.B., Tokarev, I.V., Arslanov, K.A., Druzhinin, S.V., Lyubas, A.A., Gofarov, M.Y., Kostikova, I.A., Kriauciunas, V.V., Chernov, S.B., Maksimov, F.E., Bespalaja, Y.V., Aksenova, O.V., 2015. The dating of the thermal water of subarctic hydrothermal system using isotopes of uranium, thorium and carbon. Appl. Geochem. 63, 93–104.

Manasypov, R.M., Pokrovsky, O.S., Kirpotin, S.N., Shirokova, L.S., 2014. Thermokarst lake waters across the permafrost zones of western Siberia. Cryosphere 8:1177–1193. https://doi.org/10.5194/tc-8-1177-2014.

Manasypov, R.M., Vorobyev, S.N., Loiko, S.V., Kritzkov, I.V., Shirokova, L.S., Shevchenko, V.P., Kirpotin, S.N., Kulizhsky, S.P., Kolesnichenko, L.G., Zemtzov, V.A., Sinkinov, V.V., Pokrovsky, O.S., 2015. Seasonal dynamics of organic carbon and metals in thermokarst lakes from the discontinuous permafrost zone of western Siberia. Biogeosciences 12, 3009–3028.

Matyshak, G.V., Goncharova, O.Y., Moskalenko, N.G., Walker, D.A., Epstein, H.E., Shur, Y., 2017. Contrasting soil thermal regimes in the forest-tundra transition near Nadym, West Siberia, Russia. Permafr. Periglac. Process. 28 (1):108–118. https://doi.org/10.1002/ppp.1882.

Moskalenko, N.G., 2012. Cryogenic landscape changes in the west Siberian northern taiga in the conditions of climate change and human-induced disturbances. Earth Cryosphere 16 (2), 38–42.

Mu, C.C., Abbott, B.W., Wu, X.D., Zhao, Q., Wang, H.J., Su, H., ... Zhang, T.J., 2017. Thaw depth determines dissolved organic carbon concentration and biodegradability on the northern Qinghai-Tibetan Plateau. Geophys. Res. Lett. 44, 9389–9399.

Nazarov, D.V., 2007. New data on quaternary deposits of central part of the western Siberian Arctic. Reg. Geol. Metallog. 30–31, 213–221 (In Russian).

Newmann, B.D., Throckmorton, H.M., Graham, D.E., Gu, B., Hubbard, S.S., Liang, L., Wu, Y., Heikoop, J.M., Herndon, E.M., Phelps, T.J., Wilson, C.J., Wullschleger, S.D., 2015. Microtopographic and depth controls on active layer chemistry in arctic polygonal ground. Geophys. Res. Lett. 42, 1808–1817.

Novikov, S.M., Moskvin, Y.P., Trofimov, S.A., Usova, L.I., Batuev, V.I., Tumanovskaya, S.M., Smirnova, V.P., Markov, M.L., Korotkevicth, A.E., Potapova, T.M., 2009. Hydrology of Bog Territories of the Permafrost Zone of Western Siberia. BBM publ. House, St. Petersbourg (in Russian).

Olefeldt, D., Roulet, N.T., 2012. Effects of permafrost and hydrology on the composition and transport of dissolved organic carbon in a subarctic peatland complex. J. Geophys. Res. 117, G01005. https://doi.org/10.1029/2011JG001819.

Palmer, S.M., Evans, C.D., Chapman, P.J., Burden, A., Jones, T.G., Allott, T.E.H., Evans, M.G., Moody, C.S., Worrall, F., Holden, J., 2016. Sporadic hotspots for physico-chemical retention of aquatic organic carbon: from peatland headwater source to sea. Aquat. Sci. 78, 491–504.

Panova, N.K., Antipina, T.G., Gilev, A.V., Trofimova, S.S., Zinoviev, E.V., Erokhin, N.G., 2010. Holocene dynamics of vegetation and ecological conditions in the Southern Yamal Peninsula according to the results of comprehensive analysis of a relict peat bog deposit. Russ. J. Ecol. 41 (1):20–27. https://doi.org/10.1134/S1067413610010042.

Paromov, V.V., Zemtsov, V.A., Kopysov, S.G., 2017. Climate of West Siberia during the slowing phase of warming (1986–2015) and prediction of hydro-climatic resources for 2021–2030. Bulletin of the Tomsk Polytechnic University. Geo Assets Engineering 328 (1), pp. 62–74 (in Russian with English abstract).

Pastukhov, A.V., Kaverin, D.A., 2016. Ecological state of peat plateaus in northeastern European Russia. Russ. J. Ecol. 47 (2):125–132. https://doi.org/10.1134/S1067413616010100.

Pastukhov, A.V., Marchenko-Vagapova, T.I., Kaverin, D.A., Goncharova, N.N., 2016. Genesis and evolution of peat plateaus in the sporadic permafrost area in the European northeast (middle basin of the Kosyu river). Earth Cryosphere XX (1), 3–13.

Pavlov, A.V., Moskalenko, N.G., 2002. The thermal regime of soils in the north of western Siberia. Permafr. Periglac. Process. 13:43–51. https://doi.org/10.1002/ppp.409.

Pawson, R.P., Evans, M.G., Allott, T., 2012. Fluvial carbon flux from headwater peatland streams: significance of particulate carbon flux. Earth Surf. Process. Landf. 37 (11): 1203–1212. https://doi.org/10.1002/esp.3257.

Peregon, A., Uchida, M., Shibata, Y., 2007. Sphagnum peatland development at their southern climatic range in West Siberia: trends and peat accumulation patterns. Environ. Res. Lett. 4 (4), 045014. https://doi.org/10.1088/1748-9326/2/4/045014.

Peregon, A., Uchida, M., Yamagate, Y., 2009. Lateral extension in Sphagnum mires along the southern margin of the boreal region, western Siberia. Environ. Res. Lett. 4 (4), 045028. https://doi.org/10.1088/1748-9326/4/4/045028.

Petrone, K.C., Jones, J.B., Hinzman, L.D., Boone, R.D., 2006. Seasonal export of carbon, nitrogen and major solutes from Alaskan catchments with discontinuous permafrost. J. Geophys. Res. Biogeosci. 111 (G2). https://doi.org/10.1029/2005JG000055.

Pokrovsky, O.S., Shirokova, L.S., Manasypov, R.M., Kirpotin, S.N., Kulizhsky, S.P., Kolesnichenko, L.G., Loiko, S.V., Vorobyev, S.N., 2014. Thermokarst lakes of western Siberia: a complex biogeochemical multidisciplinary approach. Int. J. Environ. Stud. 71 (5):733–748. https://doi.org/10.1080/00207233.2014.942535.

Pokrovsky, O.S., Manasypov, R.M., Shirokova, L.S., Loiko, S.V., Krickov, I.V., Kopysov, S., et al., 2015. Permafrost coverage, watershed area and season control of dissolved carbon and major elements in western Siberia rivers. Biogeosci. Discuss. 12:10621–10677. https://doi.org/10.5194/bgd-12-10621-2015.

Pokrovsky, O.S., Manasypov, R.M., Loiko, S., Krickov, I.A., Kopysov, S.G., Kolesnichenko, L.G., Vorobyev, S.N., Kirpotin, S.N., 2016a. Trace element transport in western Siberia rivers across a permafrost gradient. Biogeosciences 13:1877–1900. https://doi.org/10.5194/bg-13-1877-2016.

Pokrovsky, O.S., Manasypov, R.M., Loiko, S.V., Shirokova, L.S., 2016b. Organic and organo-mineral colloids of discontinuous permafrost zone. Geochim. Cosmochim. Acta 188: 1–20. https://doi.org/10.1016/j.gca.2016.05.035.

Polishchuk, Y.M., Bogdanov, A.N., Polischuk, V.Y., Manasypov, R.M., Shiorkova, L.S., Kirpotin, S.N., Pokrovsky, O.S., 2017. Size-distribution, surface coverage, water, carbon and metal storage of thermokarst lakes (>0.5 ha) in permafrost zone of the Western Siberia Lowland. WaterSA 9 (3):228. https://doi.org/10.3390/w9030228.

Polishchuk, Y.M., Bogdanov, A.N., Muratov, I.N., Polishchuk, V.Y., Lim, A., Manasypov, R.M., Shirokova, L.S., Pokrovsky, O.S., 2018. Minor contribution of small thaw ponds to the pools of carbon and methane in the inland waters of the permafrost-affected part of western Siberian Lowland. Environ. Res. Lett. 13 (4), 045002.

Ponomareva, O.E., Gravis, A.G., Berdnikov, N.M., 2012. Contemporary dynamics of frost mounds and flat peatlands in north taiga of West Siberia (on the example of Nadym site). Earth Cryosphere XVI (4), 21–30.

Prokushkin, A.S., Pokrovsky, O.S., Shirokova, L.S., Korets, M.A., Viers, J., Prokushkin, S.G., Amon, R., Guggenberger, G., McDowell, W.H., 2011. Sources and export fluxes of dissolved carbon in rivers draining larch-dominated basins of the central Siberian plateau. Environ. Res. Lett. 6, 045212. https://doi.org/10.1088/1748-9326/6/4/045212.

Quinton, W.L., Baltzer, J.L., 2013. The active-layer hydrology of a peat plateau with thawing permafrost (Scotty Creek, Canada). Hydrogeol. J. 21 (1):201–220. https://doi.org/10.1007/s10040-012-0935-2.

Reshetko, M.V., Moiseeva, Yu.A., 2016. Climatic features and statistical evaluation of climate change in permafrost regions in the north of Western Siberia. Bulletin Tomsk Polytechnic University. Geo Assets Eng. 327 (4), 108–118 (In Russian).

Roehm, C.L., Giesler, R., Karlsson, J., 2009. Bioavailability of terrestrial organic carbon to lake bacteria: the case of a degrading high-latitude boreal and Arctic permafrost mire complex. J. Geophys. Res. 114, G03006. https://doi.org/10.1029/2008JG000863.
Romanovsky, N.N., 1983. Underground waters of permafrost zone. Moscow University Publishing house, Moscow (in Russian).
Romanovsky, V.E., Drozdov, D.S., Oberman, N.G., Malkova, G.V., Kholodov, A.L., Marchenko, S.S., Moskalenko, N.G., Sergeev, D.O., Ukraintseva, N.G., Abramov, A.A., Gilichinsky, D.A., Vasiliev, A.A., 2010. Thermal state of permafrost in Russia. Permafr. Periglac. Process. 21:136–155. https://doi.org/10.1002/ppp.683.
Schuur, E.A.G., McGuire, A.D., Schädel, C., Grosse, G., Harden, J.W., Hayes, D.J., Hugelius, G., Koven, C.D., Kuhry, P., Lawrence, D.M., Natali, S.M., Olefeldt, C., Romanovsky, V.E., Schaefer, K., Turetsky, M.R., Treat, C.C., Vonk, J.E., 2015. Climate change and the permafrost carbon feedback. Nature 520:171–179. https://doi.org/10.1038/nature14338.
Sherstyukov, A.B., Sherstyukov, B.G., 2015. Spatial features and new trends in thermal conditions of soil and depth of its seasonal thawing in the permafrost zone. Russ. Meteorol. Hydrol. 40 (2):73–78. https://doi.org/10.3103/S1068373915020016.
Shevchenko, V.P., Pokrovsky, O.S., Vorobyev, S.N., Krickov, I.V., Manasypov, R.M., Politova, N.V., Kopysov, S.G., Dara, O.M., Auda, Y., Shirokova, L.S., Kolesnichenko, L.G., Zemtsov, V.A., Kirpotin, S.N., 2017. Impact of snow deposition on major and trace element concentrations and fluxes in surface waters of western Siberian lowland. Hydrol. Earth Syst. Sci. 21, 5725–5746.
Shirokova, L.S., Pokrovsky, O.S., Kirpotin, S.N., Desmukh, C., Pokrovsky, B.G., Audry, S., Viers, J., 2013. Biogeochemistry of organic carbon, CO_2, CH_4, and trace elements in thermokarst water bodies in discontinuous permafrost zones of western Siberia. Biogeochemistry 113, 573–593.
Shotyk, W., 1996. Peat bog archives of atmospheric metal deposition: geochemical evaluation of peat profiles, natural variations in metal concentrations, and metal enrichment factors. Environ. Rev. 4:149–183. https://doi.org/10.1139/a96-010.
Shotyk, W., Weiss, D., Kramer, J.D., Frei, R., Cheburkin, A.K., Gloor, M., Reese, S., 2001. Geochemistry of the peat bog at Etang de la Gruère, Jura Mountains, Switzerland, and its record of atmospheric Pb and lithogenic trace metals (Sc, Ti, Y, Zr, and REE) since 12,370 14C yr BP. Geochim. Cosmochim. Acta 65 (14), 2337–2360.
Shotyk, W., Rausch, N., Nieminen, T.M., Ukonmaanaho, L., Krachler, M., 2016. Isotopic composition of Pb in peat and porewaters from three contrasting ombrotrophic bogs in Finland: evidence of chemical diagenesis in response to acidification. Environ. Sci. Technol. 50:9943–9951. https://doi.org/10.1021/acs.est.6b01076.
Siegel, D.I., Reeve, A.S., Glaser, P.H., Romanovicz, E.A., 1995. Climate-driven flushing of pore water in peatlands. Nature 374:531–533. https://doi.org/10.1038/374531a0.
Smedberg, E., Mörth, C.-M., Swaney, D.P., Humborg, C., 2006. Modeling hydrology and silicon-carbon interactions in taiga and tundra biomes from a landscape perspective: implications for global warming feedbacks. Glob. Biogeochem. Cycles 20, GB2014. https://doi.org/10.1029/2005GB002567.
Smith, L.C., Macdonald, G.M., Velichko, A.A., Beilman, D.W., Borisova, O.K., Frey, K.E., Kremenetsky, K.V., Sheng, Y., 2004. Siberian peatlands as a net carbon sink and global methane source since the early Holocene. Science 303:353–356. https://doi.org/10.1126/science.1090553.
Smith, L.C., Beilman, D.W., Kremenetski, K.V., Sheng, Y., MacDonald, G.M., Lammers, R.B., Shiklomanov, A.I., Lapshina, E.D., 2012. Influence of permafrost on water storage in west Siberian peatlands revealed from a new database of soil properties. Permafr. Periglac. Process. 23:69–79. https://doi.org/10.1002/ppp.735.
Steinmann, P., Shotyk, W., 1997. Chemical composition, pH, and redox state of sulfur and iron in complete vertical porewater profiles from two Sphagnum peat bogs, Jura Mountains, Switzerland. Geochim. Cosmochim. Acta 61 (6):1143–1163. https://doi.org/10.1016/S0016-7037(96)00401-2.
Stepanova, V.M., Pokrovsky, O.S., Viers, J., Mironycheva-Tokareva, N.P., Kosykh, N.P., Vishnyakova, E.K., 2015. Major and trace elements in peat profiles in western Siberia: impact of the landscape context, latitude and permafrost coverage. Appl. Geochem. 53, 53–70.
Street, L.E., Dean, J.F., Billett, M.F., Baxter, R., Dinsmore, K.J., Lessels, J.S., Subke, J.-A., Tetzlaff, D., Wookey, P.A., 2016. Redox dynamics in the active layer of an Arctic headwater catchment; examining the potential for transfer of dissolved methane from soils to stream water. J. Geophys. Res. Biogeosci. 121:2776–2792. https://doi.org/10.1002/2016JG003387.
Sturm, M., Racine, C., Tape, K., 2001. Increasing shrub abundance in the Arctic. Nature 411:546–547. https://doi.org/10.1038/35079180.
Tape, K., Sturm, M., Racine, C., 2006. The evidence for shrub expansion in northern Alaska and the pan-Arctic. Glob. Chang. Biol. 12:686–702. https://doi.org/10.1111/j.1365-2486.2006.01128.x.
Tarnocai, C., Canadell, J.G., Schuur, E.A.G., Kuhry, P., Mazhitova, G., Zimov, S., 2009. Soil organic carbon pools in the northern circumpolar permafrost region. Glob. Biogeochem. Cycles 23, GB2023. https://doi.org/10.1029/2008GB003327.
Tetzlaff, D., Buttle, J., Carey, S.K., Mcguire, K., Laudon, H., Soulsby, C., 2015. Tracer-based assessment of flow paths, storage and runoff generation in northern catchments: a review. Hydrol. Process. 29 (16), 3475–3490.
Throckmorton, H.M., Newman, B.D., Heikoop, J.M., Perkins, G.B., Feng, X.H., Graham, D.E., Malley, D.O., Vesselinov, V.V., Young, J., Willschleger, S.D., Wilson, C.J., 2016. Active layer hydrology in an Arctic tundra ecosystem: quantifying water resources and cycling using water stable isotopes. Hydrol. Process. 30, 4972–4986.
Trofimova, I.E., Balybina, A.S., 2014. Classification of climates and climatic regionalization of the west-Siberian plain. Geogr. Nat. Resour. 35 (2):114–122. https://doi.org/10.1134/S1875372814020024.
Tyrtikov, A.P., 1973. Thawing of soils in tundra of western Siberia. In: Popov, A.I. (Ed.), Natural Environment of Western Siberia, Issue 3. Izd-vo MG, Moscow, pp. 160–169 (in Russian).
Vasil'chuk, Y., Vasil'chuk, A., Budantseva, N., Chizhova, J., 2008. Palsa of Frozen Peat Mires. Moscow University Press, Moscow (In Russian).
Vasiliev, A.A., Streletskaya, I.D., Shirokov, R.S., Oblogov, G.E., 2011. Evolution of cryolithozone of coastal zone of western Yamal during climate change. Earth Cryosphere 2, 56–64 (in Russian).
Velichko, A.A., Timireva, S.N., Kremenetski, K.V., MacDonald, G.M., Smith, L.C., 2011. West Siberian plain as a late glacial desert. Quat. Int. 237 (1–2):45–53. https://doi.org/10.1016/j.quaint.2011.01.013.
Vonk, J.E., Tank, S.E., Bowden, W.B., Laurion, I., Vincent, W.F., Alekseychik, P., Amyot, M., Billet, M.F., Canário, J., Cory, R.M., Deshpande, B.N., Helbig, M., Jammet, M., Karlsson, J., Larouche, J., MacMillan, G., Rautio, M., Walter Anthony, K.M., Wickland, K.P., 2015. Reviews and syntheses: effects of permafrost thaw on Arctic aquatic ecosystems. Biogeosciences 12:7129–7167. https://doi.org/10.5194/bg-12-7129-2015.
Walvoord, M.A., Kurylyk, B.L., 2016. Hydrological impacts of thawing permafrost – a review. Vadose Zone J. 15. https://doi.org/10.2136/vzj2016.01.0010.
Weishaar, J.L., Aiken, G.R., Bergamaschi, B.A., Fram, M.S., Fujii, R., Mopper, K., 2003. Evaluation of specific ultraviolet absorbance as an indicator of the chemical composition and reactivity of dissolved organic carbon. Environ. Sci. Technol. 37, 4702–4708.
Weiss, R.F., 1974. Carbon dioxide in water and seawater: the solubility of a non-ideal gas. Mar. Chem. 2, 203–215.
Wertebach, T.-M., Knorr, K.-H., Lordieck, M., Tretiakov, N., Blodau, C., Hölzel, N., Kleinebecker, T., 2016. Relationships between vegetation succession, pore water chemistry and CH_4 and CO_2 production in a transitional mire of western Siberia (Tyumen Oblast). Wetlands 36 (5):863–874. https://doi.org/10.1007/s13157-016-0798-8.
Weyhenmeyer, G.A., Karlsson, J., 2009. Nonlinear response of dissolved organic carbon concentrations in boreal lakes to increasing temperatures. Limnol. Oceanogr. 54 (6, part 2):2513–2519. https://doi.org/10.4319/lo.2009.54.6_part_2.2513.
White, D., Hinzman, L., Alessa, L., Cassano, J., Chambers, M., Falkner, K., Francis, J., et al., 2007. The arctic freshwater system: changes and impacts. J. Geophys. Res. 112, G04S54. https://doi.org/10.1029/2006JG000353.
Woo, M.-K., 2012. Permafrost Hydrology. Springer, Heidelberg Dordrecht London Ney York https://doi.org/10.1007/978-3-642-23462-0.
Yamamoto, S., Alcauskas, J.B., Crozier, T.E., 1976. Solubility of methane in distilled water and seawater. J. Chem. Eng. Data 21, 78–80.
Yang, D., Ye, B., Shiklomanov, A., 2004. Discharge characteristics and changes over the Ob River watershed in Siberia. J. Hydrometeorol. 5, 595–610.
Yang, Z., Wullschleger, S.D., Liang, L., Graham, D.E., Gu, B., 2016. Effects of warming on the degradation and production of low-molecular-weight labile organic carbon in an Arctic tundra soil. Soil Biol. Biochem. 95:202–211. https://doi.org/10.1016/j.soilbio.2015.12.022.
Yeghicheyan, D., Bossy, C., Bouhnik Le Coz, M., Douchet, Ch., Granier, G., Heimburger, A., Lacan, F., Lanzanova, A., Rousseau, T.C.C., Seidel, J.-L., Tharaud, M., Candaudap, F., Chmeleff, J., Cloquet, C., Delpoux, S., Labatut, M., Losno, R., Pradoux, C., Sivry, Y., Sonke, J.E., 2013. A compilation of silicon, rare earth element and twenty-one other trace element concentrations in the Natural River Water Reference Material SLRS-5 (NRC-CNRC). Geostand. Geoanal. Res. 37:449–467. https://doi.org/10.1111/j.1751-908X.2013.00232.x.
Zhang, T.J., Frauenfeld, O.W., Serreze, M.C., Etringer, A., Oelke, C., McCreight, J., Barry, R.G., Gilichinsky, D., Yang, D.Q., Ye, H.C., Ling, F., Chudinova, S., 2005. Spatial and temporal variability in active layer thickness over the Russian Arctic drainage basin. J. Geophys. Res.-Atmos. 110. https://doi.org/10.1029/2004JD005642.
Ziegler, S.E., Benner, R., Billings, S.A., Edwards, K.A., Philben, M., Zhu, X., Laganiére, J., 2017. Climate warming can accelerate carbon fluxes without changing soil carbon stocks. Front. Earth Sci. 5 (2). https://doi.org/10.3389/feart.2017.00002.